

People's Democratic Republic of Algeria
Ministry of Higher Education and Scientific Research
UNIVERSITY MOHAMED KHIDER, BISKRA
FACULTY of EXACT SCIENCES and NATURAL and LIFE SCIENCES
DEPARTMENT OF MATHEMATICS



Thesis submitted for the award of the Diploma :

PhD in Mathematics

Option: *Analysis*

By

ZAAMOUNE Faiza

Title :

Attractors and bifurcations of chaotic systems

Review Committee Members :

Khelfallah Nabil	Prof	University of Biskra	President
Menacer Tidjani	Prof	University of Biskra	Framer
Aissaoui Adel	Prof	University of El oued	Examiner
Guedda Lamine	MCA	University of El oued	Examiner
Laiadi abdelkader	MCA	University of Biskra	Examiner

2022

Dedicace

I dedicate this thesis to my dear husband, may God have mercy on him and make his place heaven and to my beloved family and all my friends.

THANKS

To begin with, I want to express my gratitude to Allah for giving me the courage and strength to do this simple work.

I would like to express my deep gratitude and thanks to my thesis supervisor, **Prof. T. Menacer**, Professor at Mohamed Khider Biskra University.

Carrying out my thesis under his supervision was a great honor and a real pleasure for me. His advice and encouragement guided and stimulated my work.

I deeply thank **Prof. N. Khelfallah**, Professor at Mohamed Khider Biskra University, for agreeing to chair my jury. My deepest thanks are also addressed to Mr.

-**A. Aissaoui**, Professor at the University of El Oued.

-**L. Guedda**, Lecturer at the University of El Oued.

-**A. Laiadi**, Lecturer at the University of Biskra.

To be members of the jury and having the great honor of presenting my thesis in front of them.

I take this opportunity to thank Professor **R. lozi** at University Côte d'Azur France for help me, and Professor **M. Bomehrez**, Professor **M. Hammodi** and Professor **A. Zitouni** at Mohamed Khider Biskra University in the department of electrical engineering and all my colleagues for their advices and help.

I could never forget the support of colleagues and the group administration of my establishment: big thanks.

I am very sensitive at this time to express my sincere and great thanks to all the members of my small and large family and to all my friends for their support and encouragement.

Contents

Dedicace	i
Thanks	ii
Table of Contents	iii
List of Figures	vi
Introduction	1
1 Dynamical Systems and Chaos	5
1.1 Introduction	5
1.2 Important Definitions and Notations	6
1.2.1 Phase Space	7
1.2.2 Conservative Systems and Dissipative Systems	8
1.2.3 The Poincare Map	8
1.2.4 Critical Points	8
1.2.5 Attractors of Dissipative Systems	10
1.3 Qualitative Study of Dynamic Systems	13
1.3.1 Linearization of Dynamic Systems	13
1.3.2 Concept of Stability	14
1.3.3 Hartmann-Grobman Theorem	17

1.3.4	Central Manifold Theorem	17
2	Bifurcation Theory	22
2.1	Introduction	22
2.2	Bifurcations in Codimension 1	23
2.3	Chaos theory	30
2.3.1	Chaos Properties	31
2.3.2	Lyapunov's Exponents	32
2.3.3	Paths to Chaos	33
3	Hidden Attractors	35
3.1	Introduction	35
3.2	Self-Excited Attractors	37
3.3	Hidden Oscillations	38
3.4	Analytical-Numerical Method for Hidden Attractor Localization	42
3.4.1	Example (Hidden Attractor for Chua's System)	45
4	Hidden Modalities of Spirals of Chaotic Attractor via Saturated Function Series and Numerical Results	50
4.1	Introduction	50
4.2	1-D n-Scroll Chaotic Attractors From Saturated Function Series	51
4.3	Recovering Hidden Bifurcation in a Multispiral Chaotic Attractor	55
4.3.1	Numerical Results of Hidden Bifurcations	57
4.3.2	The Influence of the Integration Duration Procedure for Unveiling Hidden Modalities of Odd Number of Spirals	60
5	Symmetries in Hidden Bifurcation Routes to Multiscroll Chaotic Attractors Generated by Saturated Function Series	67

5.1	Introduction	67
5.2	Models and Properties of Bifurcation Routes	68
5.2.1	Numerical Calculation of Two hidden Bifurcations Routes	68
5.2.2	Maximal Attractor Range Extension and Coding Order of Spirals Appearance	70
5.3	Symmetries of the Hidden Bifurcation Routes	71
5.3.1	Basic Cell	72
5.3.2	Symmetries	72
	Conclusion	79
	Bibliography	81
	Annexe : Program in MATLAB for Hidden Bifurcation Saturated Function Series	89

List of Figures

1.1	The Poincare map.	9
1.2	The different types of stability in the sense of Lyapunov	15
1.3	Characterization of the Global Center Manifold	18
1.4	Topological classification of hyperbolic equilibria on the plane	21
2.1	Bifurcation diagram saddle-node	25
2.2	Bifurcation diagram transcritical	26
2.3	Pitchfork type bifurcations : (a) supercritical and (b) subcritical	29
2.4	Hopf diagram bifurcation	30
3.1	Localization of limit cycle in Rayleigh system	38
3.2	Numerical localization of limit cycle in van der Pol oscillator	39
3.3	Numerical localization of chaotic attractor in Lorenz system	40
3.4	The numerical localization of chaotic attractor in Chua's circuit.	41
3.5	Hidden attractor localization	49
4.1	Saturated function series with $k = 9, h = 18, p = 2, q = 2$	52
4.2	The 6-spiral attractor generated by Eqs.(4.1)and (4.2) with $k=9, h=18,$ $p=q=2$ and $a=b=c=d1=0,7$	52
4.3	The bifurcation points for $p = q = 2$	60
4.4	The bifurcation points for $p = q = 1$	61
4.5	1 spiral for $\varepsilon = 0.4$	62

4.6	The increasing number of spirals for $\varepsilon = 0.6$ and various values of $t_{stepmax}$.	63
4.7	The increasing number of spirals for $\varepsilon = 0.95$ and various values of $t_{stepmax}$	63
4.8	The increasing number of spirals for $\varepsilon = 0.98$ and various values of $t_{stepmax}$	64
4.9	The increasing number of spirals for $\varepsilon = 0.99$ and various values of $t_{stepmax}$	65
4.10	The increasing number of spirals for $\varepsilon = 1$ and various values of $t_{stepmax}$. .	66
5.1	Symmetries of the hidden bifurcation routes : $HBR_{p,q}$ and $MARE_{p,q}$, numerically computed (black) and inferred from Eqs. (5.2) and (5.3)(red) } . .	73
5.2	The increasing number of spirals of system (4.5) according to increasing ε values, when $p = 0$ and $q = 4$, $k = 10$ and $h = 20$. (a) : The first scroll for $\varepsilon = 0.41$, (b) : The second scroll on the left for $\varepsilon = 0.6$, (c) : the third scroll on the right for $\varepsilon = 0.95$. The horizontal axis is the x-axis, the vertical axis is y-axis.	74
5.3	The increasing number of spirals of system (4.5) according to increasing ε values, when $p = 0$ and $q = 4$, $k = 10$ and $h = 20$. (a) : The fourth scroll on the right for $\varepsilon = 0.985$, (b) : The fifth scroll on the right for $\varepsilon = 0.988$, (c) : the sixth scroll on the right for $\varepsilon = 0.99$. The horizontal axis is the x-axis, the vertical axis is y-axis	75
5.4	The increasing number of spirals of system (4.5) according to increasing ε values, when $p = 2$ and $q = 3$, $k = 10$ and $h = 20$. (a) : The first scroll on the right for $\varepsilon = 0.42$, (b) : The second scroll on the left for $\varepsilon = 0.6$, (c) : the third and fourth scrolls : two left-right symmetrical for $\varepsilon = 0.95$. The horizontal axis is the x-axis, the vertical axis is y-axis.	76
5.5	The increasing number of spirals of system (4.5) according to increasing ε values, when $p = 2$ and $q = 3$, $k = 10$ and $h = 20$. (a) : The fifth and sixth scrolls : two symmetrical left-right for $\varepsilon = 0.98$, (b) : The seventh scroll on the right for $\varepsilon = 0.99$. The horizontal axis is the x-axis, the vertical axis is y-axis.	77

5.6	he first scroll between -16 and 0 for the values of the parameters $p = 0$ and $q = 4$ with the parameters values $k = 9$ and $h = 18$	78
5.7	The second scroll is in symmetry with the first one, generated between 0 and 20 ($-20, 0$) for the values of the parameters $p = 0$ and $q = 4$ with the parameters values $k = 9$ and $h = 18$	78

General Introduction

Commonly, the term "dynamical systems" refers to the active area of mathematics that is at the intersection of topology, analysis, geometry, theory of measurement, and probability and that aims to understand the dynamics of a system. This study's nature varies

depending on the dynamic system under investigation, and it also depends on the techniques employed (analytical, geometric, or probabilistic).

In the past, when mechanics was taught alongside mathematics, the earliest inquiries about dynamical systems involved mechanics. The stability of the solar system is one of the main subjects that has driven mathematical research. The *KAM* theorem mirrors Lagrange's work on the subject, which consisted of interpreting the influence of bodies other than the Sun on a planet as a series of little shocks (Kolmogorov-Arnold-Moser). The Russian mathematician Alexander Lyapunov investigated the stability of motion during the 19th century as well. It presents the concept of comparing two trajectories with similar initial conditions and quantifying the difference between them; when the difference grows exponentially, this concept is known as sensitivity to the initial conditions.

The work of Lyapunov, though forgotten at first, will turn out to be crucial for understanding several parts of chaos theory. In order to anticipate meteorological occurrences, meteorologist Edward Lorenz experimented with a technique in 1963 [34]. He discovered that a small alteration to the baseline data could significantly alter the findings entirely by accident. The phenomena of sensitivity to beginning conditions has

recently been identified by Lorenz [34]. Some dynamic process models contain one or more parameters but changing the parameters could lead to qualitative and quantitative properties. This phenomenon is often called bifurcation. The additional bifurcations are simply changes in the dynamics of the invariant attractive closed curve [46]. However, with powerful resonances, multiple fixed or periodic points, including some saddle points, appear before Hopf bifurcation. The invariant closed curve from the Hopf bifurcation then interacts with the stable and unstable manifolds of the other fixed or periodic points. As a result, the stable and unstable manifolds cross one another transversally, suggesting chaotic behavior.

Systems with this property will be available starting in 1975 under the names: chaotic systems. The recent rapid growth of nonlinear science includes chaos theory as a key subfield. Chaos, a nonlinear deterministic system with complicated and unexpected behavior, was initially identified by Lorenz in 1963 [34]. Since its inception, chaos theory has been studied and developed in great detail, and one of the current research directions is the study and creation of novel chaotic systems. Three-dimensional self-excited chaotic systems composed of ordinary differential equations, such as the Lorenz, Rossler, and Chen systems [37]-[45], and several other common three-dimensional chaotic systems, are the systems that have received the most attention. Additionally, the control coefficient of the constant component can be adjusted to alter the kind of chaotic attractor. There are many different types of 3D systems without equilibrium points that are enumerated [37]-[69] (and new 4D self-oscillation [5]), some of these systems were the subject of an analysis of the dynamical properties. The linear coupling resistor of the three-dimensional self-excited oscillation system is replaced by a voltage-controlled memristor. Finding and researching uncommon simple chaotic systems with either no equilibria or with all equilibria that are stable has recently attracted interest [48]-[54]. The term "chaotic system with hidden attractors" means a system without an equilibrium point or a system with just one stable equilibrium point. This new class of attractor has only recently been identified

by Leonov et al.[31]. Any unstable equilibrium point is not next to its basin of attraction [5]. The traditional attractor is defined as a self-excited attractor in order to distinguish between the two types of attractors, whereas the hidden attractor is formed by a system without equilibria. The attraction basin of a hidden attractor does not intersect with any small neighborhood of any equilibrium point, whereas the attraction basin of a self-excited attractor will intersect with some unstable equilibrium points. This is the key distinction between hidden attractors and self-excited attractors [32]. As a result, the dynamic properties of the concealed attractor and the self-excited attractor are entirely different. A system's parameters or initial circumstances can be altered to produce hidden attractors with various topological structures. These are known as coexistence hidden attractors, and they demonstrate the system's rich and complex dynamic properties [32]-[31]-[5].

This thesis aims to study attractors and bifurcations of chaotic systems. It contains five chapters.

In the first chapter, we give basic notions of the theory of dynamic systems (critical points, attractors, notions of stability).

The second chapter, we took about bifurcation theory, as well as the characteristics of chaotic systems and the different ways of transition to chaos.

The third chapter is devoted to the investigation of hidden attractors, in which we introduce the concept of a self-excited attractor whose basin of attraction intersects any open neighborhood of an unstable fixed point. We give a history of the self-excited attractor, definitions, and some examples. Then we move to hidden oscillations (hidden attractor). We also provide historical context and definitions for hidden attractor. Finally, we present a method for detecting a hidden attractor and give a suitable example.

In the fourth chapter, the hidden modalities of spirals of chaotic attractor via saturated function series and numerical results are discussed. First, the hidden bifurcation

in the chaotic attractor, generated by function series, is shown by applying the method presented in the second chapter. Then we give the effect of the integration duration procedure on exposing hidden modalities of an odd number of spirals. Finally, we present the numerical results.

Finally, the fifth chapter is devoted to symmetries in hidden bifurcation routes to multiscroll chaotic attractors generated by saturated function series. This includes examples and properties of bifurcation routes; contains a numerical computation of two hidden bifurcation routes; and maximal attractor range extension and coding order of spirals' appearance. Finally, we present the symmetries of the hidden bifurcation routes. At the end, one finds the bibliography used for this thesis.

Chapter 1

Dynamical Systems and Chaos

1.1 Introduction

Dynamical systems theory is a classical branch of mathematics introduced by Newton around 1665. It provides mathematical models for systems evolving over time and following rules generally expressed in analytical form as a system of ordinary differential equations. These models are called "dynamic systems continuous". In the 1880, Poincare found it convenient to replace certain dynamical systems with discrete dynamical systems.

That is, systems in which time evolves by breaks in regular sequences. Thus, for more than a hundred years, dynamical systems have been defined into two classes: continuous and discrete systems. Historically, dynamical systems developed and specialized during the 19th century.

Indeed, during the astronomical study of the three-body problem near the end of the twentieth century, the French mathematician, physicist, and philosopher Henri Poincaré had already highlighted the phenomenon of stability at the initial conditions. One or more parameters may be present in some dynamic process models, but modifying the parameters may result in qualitative and quantitative features. This occurrence is frequently known as a bifurcation [46]-[22]. Lyapunov's works, which were initially forgotten, will later be

very useful for studying certain aspects of chaos theory. In 1963, meteorologist Edward Lorenz experimented with a method that allowed him to predict weather phenomena [34].

1.2 Important Definitions and Notations

A dynamical system described by a mathematical function presents two types of variables: dynamic and static. Dynamic variables are fundamental quantities that change over time; static variables, also called parameters of the system, are fixed.

Definition 1.2.1 *The vector field F , given in a region M of the space \mathbb{R}^m , is the correspondence which compares every point $x \in M$ with the vector F of the space \mathbb{R}^m applied to this point.*

The system of differential equations, corresponding to a vector field F , is

$$\frac{dx}{dt} = F(x, \mu), \quad x \in M \subset \mathbb{R}^m, \quad \mu \in \mathbb{R}^r, \quad m \text{ et } r \in \mathbb{N}. \quad (1.1)$$

* where the point above the letter means differentiation on t . Region M is called the phase space of the system, and the direct product $I \times M$ the expanded phase space where I is an interval of the real axis of time t . The system (1.1) is also called an autonomous system of ordinary differential equations.

* We can always transform a non-autonomous system into an autonomous system.

Example 1.2.1 *We consider a system of differential equations*

$$\begin{cases} \dot{x} = y \\ \dot{y} = x - x^3 - ay + b \cos \tau s \end{cases}, \quad (x, y) \in \mathbb{R}^2.$$

where the parameters a, b, τ , are real physical.

Definition 1.2.2 *In the case where time is discrete, the dynamical system is presented by an application (iterative function)*

$$x_{k+1} = F(x_k, \mu), \quad x_k \in M \subset \mathbb{R}^m, \quad \mu \in \mathbb{R}^r \quad k = 1, 2, 3, \dots \quad (1.2)$$

Example 1.2.2 *We consider the discrete dynamical system*

$$x_{n+1} = rx_n(1 - x_n), \quad x \in [0,1].$$

1.2.1 Phase Space

We will always try to introduce the properties of dynamical system in geometrical images since this smooths their understanding. The orbits in the state space of a dynamical system $F(x, \mu)$ and the phase portrait of these orbits are the basic geometrical objects associated with it.

Definition 1.2.3 *A graph of a solution of a system of differential equations is called its integral curve, and a projection of an integral curve on phase space along the axis t is called a phase curve (trajectory, orbit).*

Definition 1.2.4 *A limit cycle is called orbitally asymptotically stable (or simply stable) if for any reason in its small neighbourhood U , all trajectories beginning in a small neighbourhood of the cycle do not leave in time and tend to the cycle when $t \rightarrow +\infty$*

Definition 1.2.5 *The phase curve (trajectory) of the periodic solution of the system (1.1) is closed and called a cycle. Back, any cycle (the closed phase curve) of the systems (1.1) defines the periodic solution of the system with some period.*

1.2.2 Conservative Systems and Dissipative Systems

For physicists, a conservative system is a system that conserves total energy. On the other hand, a dissipative system is a system that dissipates energy. So the conservative system has a first (or constant) integral of the motion, and the second has at least one rate-dependent term. But let's not forget that the systems considered are deterministic systems. So to specify this definition, we arrive at saying that a deterministic system is conservative if and only if the dynamics of the system is associated with each initial condition x_0 one and only one final state $x(t)$. It is necessary that there exists a one-to-one map φ of the phase space

$$\begin{aligned}\varphi : X \times \mathbb{R} &\rightarrow X, \\ (x, t) &\rightarrow \varphi_t(x) = \varphi(x, t).\end{aligned}\tag{1.3}$$

1.2.3 The Poincare Map

Probably the most basic tool for studying the stability and bifurcations of periodic orbits is the Poincare map or first return map, defined by Henri Poincare in 1881. The idea of the Poincare map is quite simple : If r is a periodic orbit of the system (1.1) through the point x_0 and Σ is a hyperplane perpendicular to r at x_0 , then for any point $x \in \Sigma$ sufficiently near x_0 , the solution of (1.1) through x at $t = 0$, $\phi_t(x)$, will cross Σ again at a point $P(x)$ near x_0 see figure (1.1).

Definition 1.2.6 *The mapping $x \rightarrow P(x)$ is called the Poincare map.*

1.2.4 Critical Points

Definition 1.2.7 *Let x_0 is called a equilibrium point of a differentiable vector field $F(x)$ so $F(x_0) = 0$.*

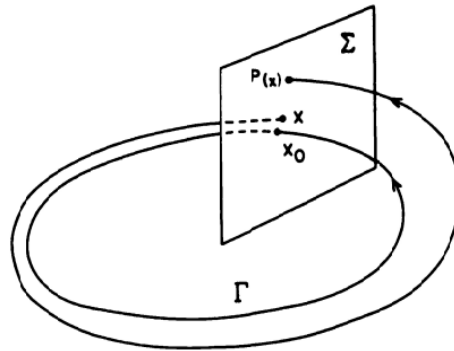


Figure 1.1: The Poincaré map.

Definition 1.2.8 *The singular point of a vector field is a point in phase space in which the vector of a field vanishes.*

Definition 1.2.9 *The periodic solution x_t of an autonomous system of differential equations (1.1) exists if there exists a constant $T > 0$, such that $x_{t+T} = x_t$ for all t . The period of the solution x_t is named after the minimal such value T and the solution x_t is called T -periodic solution.*

Definition 1.2.10 *The stationary solution of an autonomous system of differential equations (the solution which is identically equal to a singular point) is called Lyapunov stable if all solutions of this system with initial conditions from a sufficiently small neighbourhood of the singular point are defined on all positive semi-axis of time and uniformly on time converge to the investigated stationary solution when the initial conditions tend to the indicated singular point.*

Definition 1.2.11 *The isolated closed trajectory is called a limit cycle of an autonomous system of ordinary differential equations.*

1.2.5 Attractors of Dissipative Systems

As it was already mentioned above, the basic distinctive property of a dissipative system of ordinary differential equations is the compression of its phase volume in time. As a result, when $t \rightarrow \infty$, all solutions of such a system or a part of solutions tend to some compact (closed and limited) subset B of phase space M , named an attractor. Thus, the attractor contains "the set of established regimes" of the system. Now there is no generally accepted strict definition of "attractor". It is connected first of all with the reason that, till now, it is not clear what an irregular (chaotic or any other) attractor is and how it is arranged.

Definition 1.2.12 *In relation to a flow φ^t set $B \subset M$, compact invariant. If there is an attractive set in its neighbourhood U (the open set containing B) such, that $B \subset \omega(U)$ and for almost all*

$$x \in U, \varphi^t(x) \rightarrow B \text{ when } t \rightarrow \infty \text{ (i.e. } \text{dist}(\varphi^t(x), B) = \inf_{y \in B} \|\varphi^t(x) - y\| \rightarrow 0 \text{ when } t \rightarrow \infty).$$

The greatest set, U , satisfying this definition, is called a attraction of field for B .

Definition 1.2.13 *A set is called indecomposable if for any disjiont subsets $A, B \subset E$ such that $A \cup B = E$ we have $\text{Per}(E) = \text{Per}(A) + \text{Per}(B)$ then either $|A| = 0$ or $|B| = 0$.*

Definition 1.2.14 *The indecomposable attractive set is called an attractor.*

Not all attractive sets are attractors, but only those of them which possess the property of indecomposability into two separate compact invariant subsets.

Different Types of Attractors

There are two types of attractors: regular attractors and strange attractors, or chaotic attractors.

1. Regular Attractors

Regular attractors characterize the evolution of non-chaotic systems and can be of three kinds.

- **The Fixed Point**

This is the most popular case and the simplest attractor, in which the system evolves towards a point. Note that only the basins can be attractors. The other types of fixed points indeed always have at least one "output trajectory" to each eigenvalue of the Jacobian of the positive real part is associated an eigenvector that points in a direction where the phase trajectory is moving away from the fixed point.

- **The Periodic Limit Cycle**

It may happen that the phase trajectory closes in on herself. The temporal evolution is then periodic, the system presenting permanent oscillations. In a dissipative physical system, this requires the presence of a term of forcing in the equations which comes to compensate on average for the losses by dissipation.

- **The pseudo-Periodic Limit Cycle(Invariant Tori)**

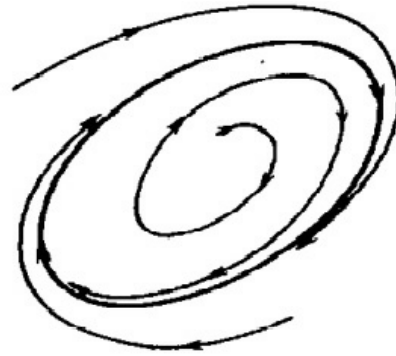
It is almost a special case of previous case. The system offers at least two simultaneous periods whose rate is irrational. The phase trajectory does not close in on itself but wraps around a 2-dimensional manifold.

2. Strange Attractors

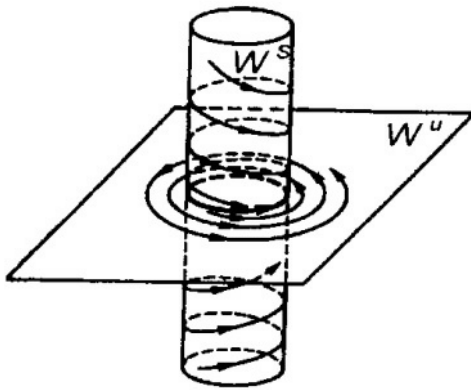
The surface containing the divergent trajectories is called an unstable manifold, while the one containing convergent trajectories will be called a stable manifold. Note that this cannot be conceived in a phase space of at least three dimensions. Strange attractors are characteristics of the evolution of chaotic systems: after a certain time, all the points in the phase space (and belonging to the basin of attraction of the attractor) give trajectories that tend to form the strange attractor.



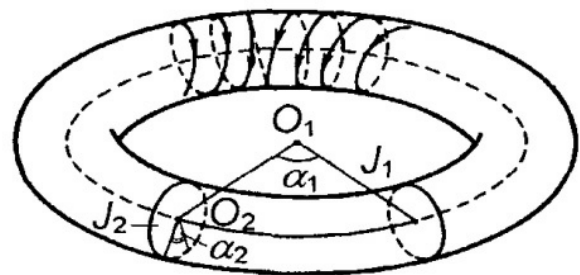
Fixed point



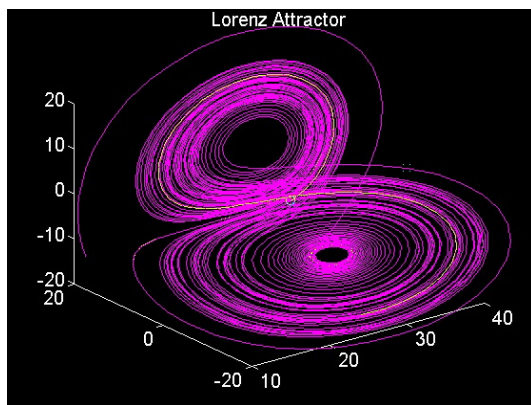
limit cycle



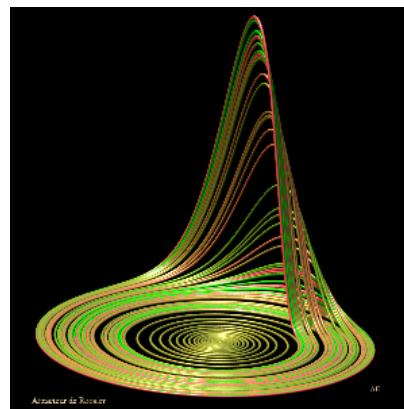
A limit cycle in natural space



Invariant tori



Lorenz Strange Attractor



Rosler Strange Attractor

1.3 Qualitative Study of Dynamic Systems

The qualitative study makes it possible to see the behavior of the solutions without having to solve the differential equation. In particular, it allows the local study of solutions around equilibrium points. To have a complete study of a dynamic system, we are waiting for, in general, from the environment, a stationary behavior. The latter will be presented by the disappearance of transitional phenomena by canceling the function of transition or vector field. In this case, the system will have one of the two states.

* The case of equilibrium (fixed points, periodic points).

* The case of chaotic

To make this study easier, the properties of linear algebra are used on equations that describe our dynamic systems, but the majority of dynamic systems associated with natural phenomena are not linear. For this purpose, we are obliged to linearize.

1.3.1 Linearization of Dynamic Systems

Consider the nonlinear dynamic system defines by:

$$\dot{X} = F(X), \quad X = (x_1, x_2, \dots, x_n), \quad F = (f_1, f_2, \dots, f_n), \quad (1.4)$$

where X_0 a fixed point (equilibrium) of this system.

Suppose a small upset $\varepsilon(t)$ is applied in the neighborhood of the fixed point. The function f can be developed in a series of Taylor in the neighborhood of point X_0 as follows:

$$\varepsilon(t) + X_0 = F(\varepsilon(t) + X_0) \simeq F(X_0) + J_F(X) \cdot \varepsilon(t), \quad (1.5)$$

with $J_F(X_0)$ is the Jacobian matrix of the function F defined by

$$J_F(X_0) = \begin{pmatrix} \frac{\partial f_1}{\partial x_1} & \frac{\partial f_1}{\partial x_2} & \dots & \frac{\partial f_1}{\partial x_n} \\ \dots & \dots & \dots & \dots \\ \frac{\partial f_n}{\partial x_1} & \frac{\partial f_n}{\partial x_2} & \dots & \frac{\partial f_n}{\partial x_n} \end{pmatrix}_{X=X_0} . \quad (1.6)$$

As $F(X_0) = X_0$, then equation (1.5) becomes again:

$$\varepsilon(t) = J_F(X_0).\varepsilon(t). \quad (1.7)$$

The writing (1.7) means that the system (1.4) is linearized.

1.3.2 Concept of Stability

Stability in The Sense of Lyapunov

Consider the following dynamic system:

$$\frac{dx}{dt} = f(x, t), \quad (1.8)$$

with f a nonlinear function

Definition 1.3.1 *The equilibrium point x_0 of the system (1.8) is:*

1. **Stable** if

$$\forall \varepsilon > 0, \exists \delta > 0 : \|x(t_0) - x\| < \delta \Rightarrow \|x(t, x(t_0)) - x_0\| < \varepsilon, \forall t \geq t_0. \quad (1.9)$$

2. **Asymptotically stable** if:

$$\exists \delta > 0 : \|x(t_0) - x\| < \delta \Rightarrow \lim_{t \rightarrow \infty} \|x(t, x(t_0)) - x_0\| = 0. \quad (1.10)$$

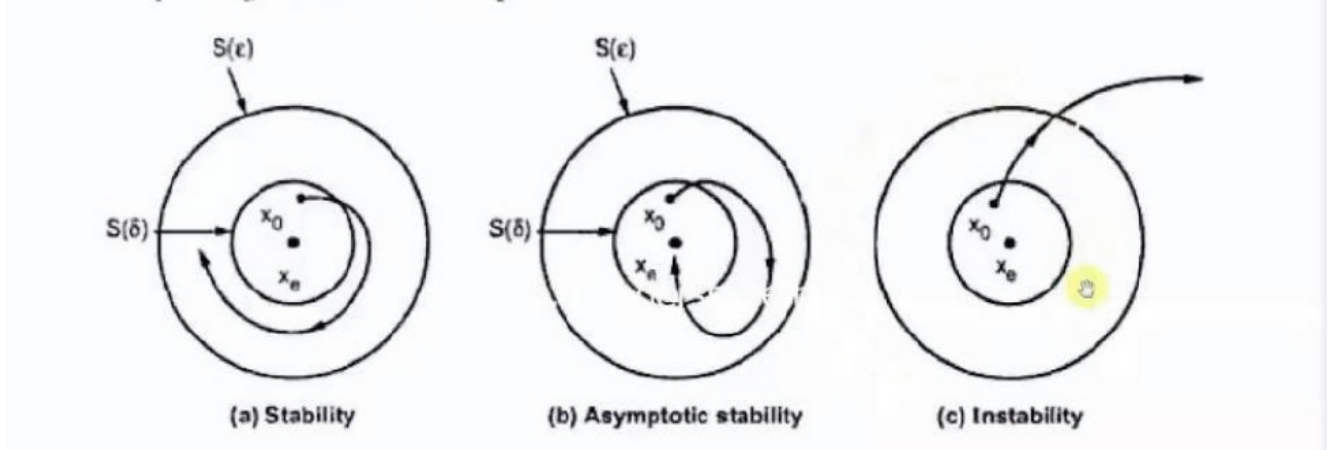


Figure 1.2: The different types of stability in the sense of Lyapunov

3. *Exponentially stable if:*

$$\forall \epsilon > 0, \exists \delta > 0 : \|x(t_0) - x\| < \delta \Rightarrow \|x(t, x(t_0)) - x_0\| < a \exp(-bt), \quad \forall t > t_0. \quad (1.11)$$

4. *Unstable if*

$$\exists \epsilon > 0, \forall \delta > 0 : \|x(t_0) - x\| < \delta \text{ and } \|x(t, x(t_0)) - x_0\| > \epsilon, \quad \forall t \geq t_0, \quad (1.12)$$

wich mean that equation (1.9) is not satisfied.

Lyapunov's First Method (Indirect Method)

Lyapunov's first method is based on examining the linearization around the equilibrium point x_0 of the system (1.8). More precisely, we examine the eigenvalues λ_i of the Jacobian matrix evaluated at the equilibrium point. According to this method, the properties of stability of x_0 are expressed as follows:

- 1- If all the eigenvalues of the Jacobian matrix have a strictly negative real part, then x_0 is exponentially stable.

2- If the Jacobian matrix has at least one eigenvalue with a strictly positive real part, x_0 is unstable.

Remark 1.3.1 *This method does not allow us to say if the equilibrium is stable or unstable when the matrix Jacobian has at least one zero eigenvalue and no eigenvalue with an exactly positive real part. In this case, the trajectories of the system converge to a subspace (a manifold) whose dimension is the number of zero eigenvalues of the Jacobian matrix and the stability of the equilibrium can be studied in this subspace by the second method.*

Lyapunov's Second Method (Direct Method)

As we have seen, Lyapunov's first method is simple to apply, but it allows us to analyze the stability of equilibria only very partially. Besides, she gives no indication of the size of the basins of attraction. The second method is more difficult to implement, but, on the other hand, it is far-reaching and more general. It is founded on the definition of a specific function, denoted $V(x)$ and known as the Lyapunov function, which decreases along the trajectories of the system within the attraction basin. This theorem will summarize this method.

Theorem 1.3.1 *The system's equilibrium point x_0 (1.8) is stable if a function $V(x) : D \rightarrow \mathbb{R}$ continuously differentiable having the following properties :*

1. D is an open of \mathbb{R}^n and $x_0 \in D$,
2. $V(x) > V(x_0) \forall x \neq x_0$ in D ,
3. $\dot{V}(x) \leq 0 \forall x \neq x_0$ in D .

There is no method to find a Lyapunov function. But in mechanics and for electrical systems, one can often use the total energy as a Lyapunov function.

1.3.3 Hartmann-Grobman Theorem

Consider the dynamical system (1.4).

Let X_0 be an equilibrium point of the system (1.4) and let $J_F(X)$ be the Jacobian matrix at point X_0 .

The following theorem follows:

Theorem 1.3.2 *If $J_F(X_0)$ admits pure non-zero or imaginary eigenvalues, then there exists a homeomorphism which transforms the orbits of the nonlinear flow into those of the flow linear in some neighborhood U of X_0 . This theorem will allow us to link the dynamics of the nonlinear system (1.4) to the dynamics of the linearized system (1.7) .*

1.3.4 Central Manifold Theorem

Let's

$$\frac{dx}{dt} = f(x, c), \quad (1.13)$$

a nonlinear dynamic system, x_0 is a point of equilibrium which can be brought back to the origin by the change of a variable :

$$\varrho = x - x_0,$$

and let J be the Jacobian matrix of order n associated with the system (1.13) after its linearization in the neighborhood of the fixed point (after having considered a small perturbation ϱ in the neighborhood of the fixed point)

$$\frac{d\varrho}{dt} = J\varrho.$$

Where :

- N^s the vectorial subspace of dimension s is generated by $\{\lambda_1, \lambda_2, \dots, \lambda_s\}$.

- N^i the vectorial subspace of dimension i is generated by $\{u_1, u_2, \dots, u_i\}$.
- N^c the vectorial subspace of dimension c is generated by $\{s_1, s_2, \dots, s_c\}$.

With

$$N^n = N^s \oplus N^i \oplus N^c.$$

And where :

- * $\lambda_1, \lambda_2, \dots, \lambda_s$ the eigenvalues of the Jacobian matrix J , whose part real is negative.
- * u_1, u_2, \dots, u_i the eigenvalues of the Jacobian matrix J , whose real part is positive.
- * s_1, s_2, \dots, s_c the eigenvalues whose real part is zero, with $s + i + c = n$.

We have the following theorem :

Theorem 1.3.3 *There are manifolds of class C^r : T^s stable, T^i unstable and T^c central tangents respectively to N^s , N^i and N^c in x_0 . These manifolds are invariant with respect to the flow system (1.13).*

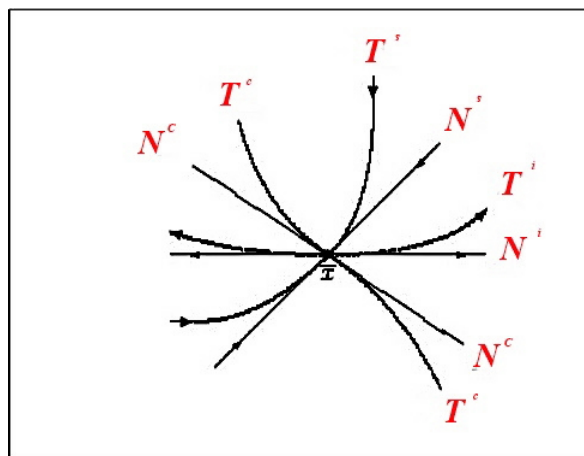


Figure 1.3: Characterization of the Global Center Manifold

Central Manifold Depending on a Parameter

We apply a small perturbation χ to the system (1.13), so the result will be a dynamical system depending on a parameter χ , and suppose that by a certain transformation we can reduce the system (1.13) to a system of the form :

$$\begin{cases} \dot{x} = A_1x + f(x, y, z, \chi), \\ \dot{y} = A_2y + g(x, y, z, \chi), \\ \dot{z} = A_3z + h(x, y, z, \chi), \\ \dot{\chi} = 0. \end{cases} \quad (1.14)$$

The central manifold in the neighborhood of $(0, 0, 0, 0)$ is then given by :

$$y = k_1(x, \chi), \quad z = k_2(x, \chi).$$

After a simple calculation and after having applied the Taylor expansion on k_1 and k_2 , we can write the system (1.14) under the form :

$$\begin{cases} \dot{x} = A_1x + f(x, k_1(x, \chi), k_2(x, \chi), \chi) \\ \dot{\chi} = 0 \end{cases} \quad (1.15)$$

The following theorem makes it possible to link the dynamics of the system (1.15) to that of the system (1.14):

Theorem 1.3.4 *If the origin $x_0 = 0$, of the system (1.15) is asymptotically stable (unstable), then the origin of the system (1.14) is also asymptotically stable (unstable).*

Poincare Classification of Fixed Points

It is about distinguishing these fixed points by the nature of the eigenvalues of the matrix Jacobian (1.6) of the linearized system (1.7) associated with the initial differential system (1.4) at this point.

For this reason, we will assume that the eigenvalues of the matrix Jacobian (1.6) are defined by:

$$\lambda_i = \omega_i + j\sigma_i, \quad i = 1, 2, \dots, n.$$

During $\omega_i \neq 0$ for $i = 1, 2, \dots, n$ the fixed point is said to be hyperbolic.

The solution $\varepsilon(t)$ of the linearized system is written on the basis of autonomous functions:

$$\varepsilon(t) = \sum_{i=1}^n C_i \exp(\lambda_i t) \cdot V_i. \quad (1.16)$$

Where V_i represents the eigenvector associated with λ_i and $C_i \in \mathbb{R}$ depends on the initial conditions.

So the eigenvalues λ_i define the state of stability.

And we will cite the nature of these fixed points by studying the nature of the λ_i .

1/ If $\omega_i < 0$ for $i = 1, 2, \dots, n$, the fixed point is asymptotically stable : $\lim_{t \rightarrow +\infty} y(t) = 0$.

The point is said to be a **focus** if $\sigma_i \neq 0$ for $i = 1, 2, \dots, n$, a **node** if $\sigma_i = 0$ for $i = 1, 2, \dots, n$.

2/ If $\omega_i > 0$ for $i = 1, 2, \dots, n$, the fixed point is unstable. We say that the point is a **source** if $\sigma_i \neq 0$ for $i = 1, 2, \dots, n$, and a **node** if $\sigma_i = 0$ for $i = 1, 2, \dots, n$.

3/ If $\omega_j > 0$ for $j = 1, 2, \dots, p$ with $p < n$ and $\omega_j < 0$ for $i \neq j$, the solution is unstable, and the point is a saddle.

If there is no zero eigenvalue, we have a saddle point.

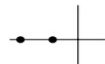
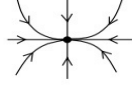
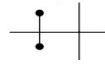


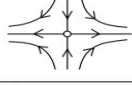

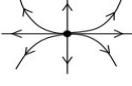


(n_+, n_-)	Eigenvalues	Phase portrait	Stability
(0, 2)		 node	stable
		 focus	
(1, 1)		 saddle	unstable
(2, 0)		 node	unstable
		 focus	

Figure 1.4: Topological classification of hyperbolic equilibria on the plane

Chapter 2

Bifurcation Theory

2.1 Introduction

The case in which we are interested in this part is as follows: we consider a differential system depending on auxiliary parameters and we want to understand what modifications of form undergo the portrait of phases when the parameters vary. This is the question that the theory of disasters answers when we restrict ourselves to the framework of dissipative systems depending on potential and when we only take into account as significant characteristics of the portrait of phases the positions of equilibria and their bifurcations. For the values of the parameters at which such qualitative changes appear, so called bifurcation values (see [22]), the construction of the phase portrait requires appropriate tools. We are interested here in local bifurcations, relative to a point of equilibrium of a continuous system, and the bifurcation diagram will help us geometrically with both methods, which brings us back to the use of good coordinates:

- * The method of the central sub-manifold makes it possible to isolate the non-hyperbolic part, called the central, of the system.
- * Only true nonlinearities, those that cannot be made to disappear by regular coordinate changes, remain in Poincaré's method of normal forms.

Definition 2.1.1 *Defining a nonlinear dynamic system*

$$\frac{dx}{dt} = g(x, t, \tau). \quad (2.1)$$

Let x_0 be the solution to the problem of dimension n and control parameter τ .

A bifurcation is a qualitative change of the solution x_0 of the system (2.1) when we modify τ , and more precisely, the disappearance or the change of stability and the appearance of new solutions.

Definition 2.1.2 *The minimum number of parameters needed for a universal unfolding is called the codimension of the singularity. The codimension of the bifurcation indicates how many parameters the system of differential equations should have on which the bifurcation was exemplary. If codimension is greater than one, a bifurcation occurs that is more irregular for the system.*

Definition 2.1.3 *A bifurcation diagram is a portion of the parameter space on which all the bifurcation points are represented.*

2.2 Bifurcations in Codimension 1

We are talking here only about the bifurcation of codimension 1, and there are four types of bifurcation of codimension 1, which all correspond to generic behaviors.

a- Saddle-Node Type Bifurcation

A linear function does not change the number of roots. The simplest polynomial which changes the number of roots depending on the parameter τ is the quadratic polynomial.

Consider the following one-dimensional dynamical system depending on one parameter:

$$g(x, \tau) = \tau - x^2. \quad (2.2)$$

We call the function (2.2) the normal form of the saddle-node bifurcation.

We will investigate the behavior of this equation in relation to the control parameter τ :

$$g(x, \tau) = 0 \iff \tau - x^2 = 0,$$

$$\tau - x^2 = 0 \iff \tau = x^2.$$

1. If $\tau < 0$, the equation $g(x, \tau) = 0$, as no solution. So there is no point of equilibrium.
2. If $\tau > 0$, we have :

$$x^2 = \tau \iff \begin{cases} x_1 = \sqrt{\tau}, \\ x_2 = -\sqrt{\tau}. \end{cases}$$

Therefore, equation (2.2) has two solutions, so there are two equilibrium points.

Their stability is determined by :

$$\frac{dg(x, \tau)}{dx} = -2x \text{ so } \frac{dg(x, \tau)}{dx} \Big|_{x_1} = -2\sqrt{\tau} < 0 \text{ and } \frac{dg(x, \tau)}{dx} \Big|_{x_2} = 2\sqrt{\tau} > 0.$$

As a direct result, the signs $\frac{dg(x, \tau)}{dx} \Big|_{x_{1,2}}$, we see that :

$$\begin{cases} x_1 \text{ is stable,} \\ x_2 \text{ is is unstable.} \end{cases}$$

Remark 2.2.1 *Same study done when $g(x, \tau) = -\tau - x^2$, $g(x, \tau) = \tau + x^2$, $g(x, \tau) = -\tau + x^2$.*

But in all cases, there is a transition at $\tau = 0$ between the existence of no fixed point and the existence of two fixed points, one of which is stable and the other unstable.

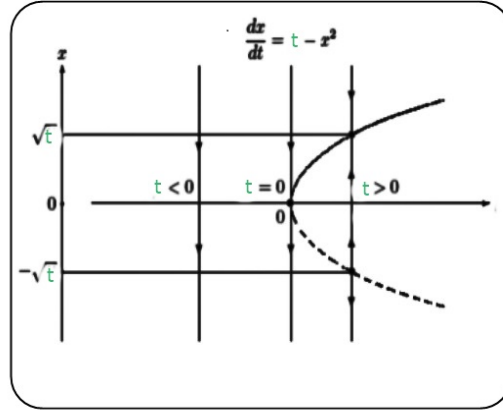


Figure 2.1: Bifurcation diagram saddle-node

b- Transcritical Type Bifurcation

If g is constrained to have no constant term, the bounded expansion leads to the normal form of a transcritical bifurcation, which is the last stationary bifurcation in one dimension:

$$g(x, \tau) = \tau x - x^2. \quad (2.3)$$

The usual analysis gives :

$$g(x, \tau) = 0 \iff \tau x - x^2 = 0 \iff x(\tau - x) = 0.$$

$$\begin{cases} x_1 = 0, \\ x_2 = \tau. \end{cases}$$

The equation $g(x, \tau) = 0$ admits two equilibrium points

$$\frac{dg(x, \tau)}{dx} \Big|_{x_1=0} = \tau \quad \text{and} \quad \frac{dg(x, \tau)}{dx} \Big|_{x_2=\tau} = -\tau.$$

So: the equilibrium point $x_1 = 0$ stable for $\tau < 0$, unstable for $\tau > 0$ and $x_2 = \tau$ and stable for $\tau > 0$, unstable for $\tau < 0$.

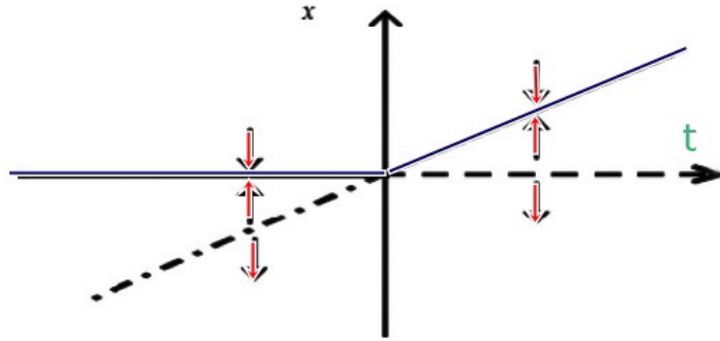


Figure 2.2: Bifurcation diagram transcritical

c- Pitchfork Type Bifurcation

At the pitchfork bifurcation point, the stability of an equilibrium point changes in favor of the birth of a pair of equilibrium points. There are two kinds of this bifurcation : supercritical, having a normal form:

$$g(x, \tau) = \tau x - x^3. \quad (2.4)$$

And subcritical, having a normal form :

$$g(x, \tau) = \tau x + x^3.$$

We calculate the equilibrium points. In the case of a supercritical pitchfork bifurcation, we have

$$\begin{aligned} g(x, \tau) &= 0, \\ \tau x - x^3 &= 0 \Leftrightarrow x(\tau - x^2) = 0. \end{aligned}$$

$$\Leftrightarrow \begin{cases} x = 0 \\ \text{ou} \\ \tau - x^2 = 0 \end{cases} \Leftrightarrow \begin{cases} x = 0, \\ \text{ou} \\ x^2 = \tau. \end{cases}$$

So, if $\tau < 0$, we have a single point of equilibrium at $x = 0$.

If $\tau > 0$, we have three equilibrium points

$$\begin{cases} x_1 = 0, \\ x_{2,3} = \pm\sqrt{\tau}. \end{cases}$$

We study the stability of these equilibrium points:

$$\frac{dg(x, \tau)}{dx} = \tau - 3x^2 \text{ so } \begin{cases} \frac{dg(x, \tau)}{dx} \Big|_{x_1} = \tau, \\ \frac{dg(x, \tau)}{dx} \Big|_{x_{2,3}} = -2\tau. \end{cases}$$

As a result :

- If $\tau < 0$ we have the only equilibrium point where $x = 0$ is stable.
- If $\tau > 0$ we have the equilibrium point:

$$\begin{cases} x = 0 \text{ is unstable,} \\ x = \pm\sqrt{\tau} \text{ is stable.} \end{cases}$$

- if $\tau = 0$ we have a single point of equilibrium where $x = 0$ is semi-stable.

In the case of a subcritical pitchfork bifurcation, the same calculation yields

$$\begin{aligned} g(x, \tau) &= 0, \\ \tau x + x^3 &= 0 \Leftrightarrow x(\tau + x^2) = 0. \end{aligned}$$

$$\Leftrightarrow \left\{ \begin{array}{l} x = 0 \\ \text{ou} \\ \tau + x^2 = 0 \end{array} \right. \Leftrightarrow \left\{ \begin{array}{l} x = 0, \\ \text{ou} \\ x^2 = -\tau. \end{array} \right.$$

So, if $\tau > 0$, we have a single point of equilibrium $x = 0$.

If $\tau < 0$, we have three equilibrium points

$$\left\{ \begin{array}{l} x_1 = 0, \\ x_{2,3} = \pm\sqrt{-\tau}. \end{array} \right.$$

We study the stability of these equilibrium points :

$$\frac{dg(x, \tau)}{dx} = \tau + 3x^2 \text{ so } \left\{ \begin{array}{l} \frac{dg(x, \tau)}{dx} \Big|_{x_1=0} = \tau, \\ \frac{dg(x, \tau)}{dx} \Big|_{x_{2,3}} = -2\tau. \end{array} \right.$$

As a result :

- If $\tau > 0$ we have the only equilibrium point where $x = 0$ is unstable.
- If $\tau < 0$ we have the equilibrium point:

$$\left\{ \begin{array}{l} x = 0 \text{ is stable,} \\ x = \pm\sqrt{-\tau} \text{ is unstable.} \end{array} \right.$$

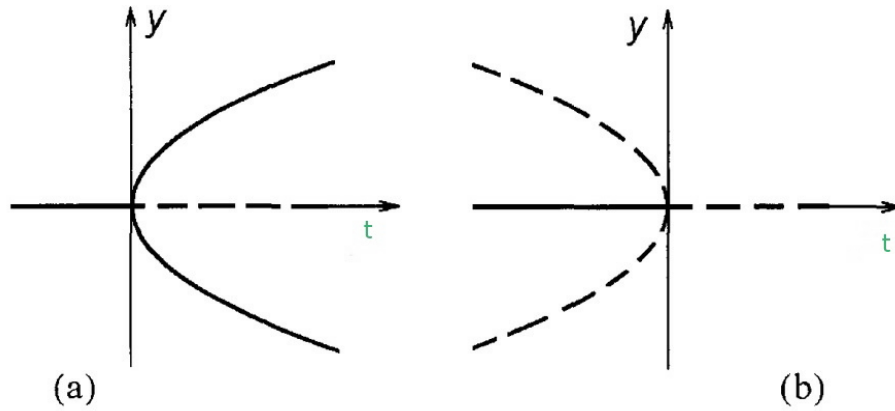


Figure 2.3: Pitchfork type bifurcations : (a) supercritical and (b) subcritical

d- Hopf Type Bifurcation

While all the bifurcations we have described are stationary, the Hopf bifurcation gives rise to oscillating solutions; the phase space now has two components and the shape is written in the complex plane.

Consider the normal form of Hopf type bifurcation:

$$\frac{dZ}{dt} = \tau Z - |Z|^2 Z. \quad (2.5)$$

By asking $\tau = \tau' + i\tau''$ and $Z = X \exp(i\theta)$, we get:

$$\begin{cases} \frac{dX}{dt} = \tau' X - X, \\ \frac{d\theta}{dt} = \tau''. \end{cases}$$

We therefore obtain a pitchfork bifurcation for the amplitude while the phase rotates at speed τ'' . The solution is therefore periodic, and the trajectories describe a spiral drawn towards an asymptotic curve called the limit cycle. Naturally, the bifurcation of Hopf can also be subcritical if the coefficient of the term $|Z|^2 Z$ has a positive sign, then a negative term is needed in $|Z|^4 Z$ to obtain a non-linear saturation.

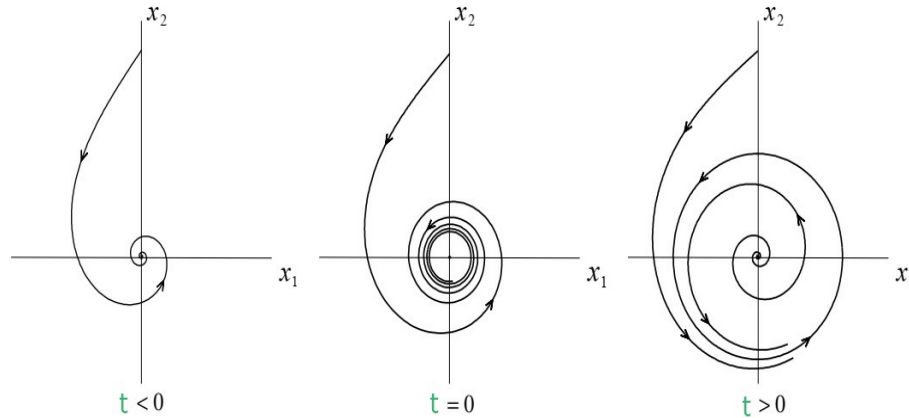


Figure 2.4: Hopf diagram bifurcation

We will now focus on the step that follows the temporal regularity. According to Landau the bifurcation of a point from a stationary behavior (equilibrium point) towards a periodic behavior (limit cycle) and then biperiodic (a torus) constitutes the first stages of the green transition turbulence. The latter presents a very interesting phenomenon that we call chaos, which has long been synonymous with disorder and confusion and is opposed to order and method. Many researchers in science have been interested in so-called chaotic movements. They confirmed that, contrary to what deterministic thought has hammered home for ages, there could be equilibrium in the disequilibrium, organization in the disorganization.

2.3 Chaos theory

Nonlinear, or simply piecewise linear, dynamic systems can exhibit completely unpredictable behaviors, which may even seem random (although these are perfectly deterministic systems). This unpredictability is called chaos. The branch of dynamical systems that endeavors to define and study chaos is called chaos theory. This branch of mathematics qualitatively describes the long-term behaviors of dynamical systems.

2.3.1 Chaos Properties

1. Sensitivity to Initial Conditions

For a chaotic system, a very small error in the knowledge of the initial state x_0 in phase space will (almost always) be rapidly amplified. From a mathematical point of view, we say that the function f shows a sensitive dependence on initial conditions when:

$$\exists \beta > 0, \forall x \in M, \forall \varepsilon > 0, \exists (y, q) \in M : \begin{cases} \|x - y\| < \varepsilon, \\ \|f^q(x) - f^q(y)\| > \beta. \end{cases} \quad (2.6)$$

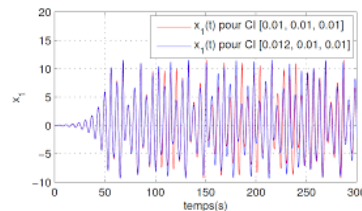
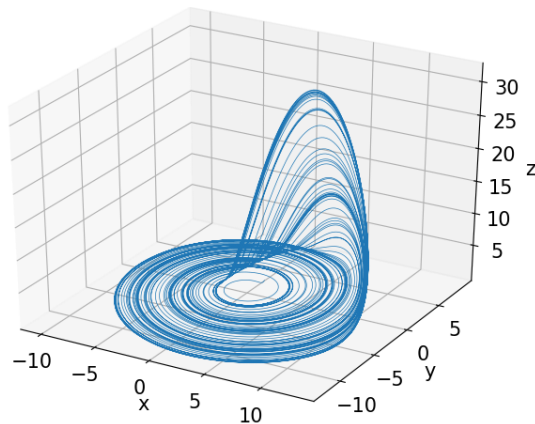
2. The Strange Attractor

A dissipative chaotic system has at least one attractor of a particular type called a strange attractor, see [37]. Geometrically, such an attractor can be described as the result of the stretching and folding operation of a phase space cycle, repeated an infinite number of times. The "length" of the attractor is infinite, although it is contained in a finite space. So we can give this definition:

Definition 2.3.1 *A bounded subset H of the phase space is a strange or chaotic attractor for a transformation P of the space if there exists a neighborhood G of H that is, for every point of H there exists a ball containing this point and contained in G satisfying the following properties.*

- a-** Attraction: G is a capture zone, which means that any orbit by P whose initial point is in G , is entirely contained in G . Moreover, any such orbit becomes and remains as close to H as one wants.
- b-** It is contained in a finite space. Its volume is zero. Its dimension is fractal (not whole).

- c- Almost any trajectory on the attractor has the property of never passing twice over the same point: each trajectory is almost surely aperiodic.
 - d- Two trajectories close at a time to see their distance locally increase at an exponential rate (sensitivity to initial conditions).
3. The existence of broad spectra is an essential characteristic of the chaotic motions of a system. The temporal evolution of a dynamic system is often represented by the value of one of its variables at regular intervals. This is called the time series.



Example of a sequence with chaotic behavior:

Chaotic behavior of the Lorenz system

2.3.2 Lyapunov's Exponents

There are several methods that can be used to determine whether nonlinear systems are chaotic or not. They are generally not very numerous nor spread over a sufficiently long time on the scale of the system studied. We chose to implement two of the most commonly used methods, which, moreover, are complementary: the fractal dimension and the Lyapunov exponents. On October 12, 1892, Lyapunov defended a doctoral thesis at the University of Moscow entitled: The General Problem of the Stability of Motion. He introduces the idea of measuring the possible divergence between two orbits resulting

from similar initial conditions. When this divergence increases exponentially with time for almost all initial conditions close to a given point, we have the phenomenon of sensitivity to the initial conditions, an idea to which the Lyapunov exponents are attached, which gives a quantitative measure of this local exponential divergence and actually measures the degree of sensitivity of a dynamic system.

2.3.3 Paths to Chaos

A dynamic system generally has one or more so-called "control" parameters, which act on the characteristics of the transition function. Depending on the value of the control parameter, the same initial conditions lead to trajectories corresponding to qualitatively different dynamic regimes. The continuous modification of the control parameters leads in many cases to a progressive complexification of the regime dynamic developed by the system. There are several scenarios that describe the transition from a fixed point to chaos. We note in all cases that the evolution from the fixed point to chaos is not progressive but marked by discontinuous changes that we have already called bifurcations.

A bifurcation marks the sudden passage from one dynamic regime to another, qualitatively different one. Three scenarios of transition to chaos can be cited:

1. **Intermittency Towards Chaos:** a stable periodic movement is interrupted by bursts of turbulence. As the control parameter is increased, the bursts of turbulence become more and more frequent, and finally, the turbulence dominates.
2. **The Period-Doubling** is characterized by a succession of bifurcations of forks. As the stress increases, the period of a forced system is multiplied by two, then by four, then by eight,..., these doublings of period are getting closer and closer; when the period is infinite, the system becomes chaotic.
3. Quasi-periodicity occurs when a second system disturbs an initially periodic system. If the ratio of the periods of the two systems in the present is not rational, then the

system is said to be quasiperiodic. In particular, Jean Christophe Yoccoz's work on dynamical systems earned him the Fields Medal in 1994.

Chapter 3

Hidden Attractors

3.1 Introduction

The analysis and synthesis of oscillating systems, for which the problem of the existence of oscillations can be solved relatively easily, received a lot of attention during the initial period of development of the theory of nonlinear oscillations in the first half of the 20th century. For example, [Andronov et al., 1966] [4], (at the end of the 19th century, this research was started in Rayleigh's (1877) [44]. The applied research on periodic oscillations in mechanics, electronics, chemistry, biology, and other fields prompted these investigations.

Numerous applied systems under consideration had structures that made the presence of oscillations "almost obvious". The oscillations were sparked by an unstable equilibrium (called selfexcited oscillation). After that, in the middle of the 20th century, it was discovered that numerically chaotic oscillations, aside from self-excited periodic oscillations, are also excited from an unstable equilibrium and can be calculated using the standard computational method [Lorenz, 1963] [34]. The computation and analysis of self-excited chaotic oscillations have recently attracted thousands of publications. The term "attractor" refers to an oscillation that attracts attention as well as a group of os-

cillations that do the same. Here, self-excited attractors and computational mathematics both naturally incorporate the ideology of transient processes from control theory. Mid-way through the 20th century, good examples of periodic and chaotic oscillations of a different sort, later referred to as "hidden oscillations" and "hidden attractors" [Leonov et al., 2011] [27], were discovered. In these oscillations, the basin of attraction does not coincide with small neighborhoods of equilibria. Since there is no way to employ equilibria information to group related transient processes in the conventional computational technique, numerical localization, computing, and analytical examination of hidden attractors are substantially more difficult challenges. As a result, this common method cannot be used to compute the hidden attractors. Additionally, since a basin of attraction might be very small and the dimension of the hidden attractor itself can be considerably less than the dimension, it is doubtful that the

integration of trajectories with random initial data can provide the localization of the hidden attractor in this instance.

The issue of analyzing hidden oscillations originally appeared in Hilbert's 16th problem for two-dimensional polynomial systems in 1900, specifically in its second section [Hilbert, 1901 – 1902] [17]. The first challenging findings were found in Bautin's writings (1939, 1952)[7]-[8]-[9], which dealt with building nested limit cycles in quadratic systems and demonstrated the importance of understanding hidden oscillations in order to solve this issue. Later, difficulties with automatic control caused by engineering led to the issue of analyzing concealed oscillations. Kapranov investigated [Kapranov, 1956] [19] the qualitative behavior of PLL systems, which are often employed in modern telecommunications and computing designs, and estimated stability domains. The issues raised spurred a wide range of study in the latter half of the 20th century. The theory of normal forms and bifurcation theory were both developed in response to Hilbert's sixteenth issue, whereas the idea of absolute stability was developed in response to the Aizerman problem [1].

The authors' Kuznetsov et al., 2010; Leonov et al., 2010 [28] (first-time) discovery of

a chaotic hidden attractor in a generalized Chua's circuit and subsequent discovery of a chaotic hidden attractor in a classical Chua's circuit [Leonov et al., 2011] [27], this greatly encouraged further research into hidden oscillations. It needs to be noted that Chua's circuit and its numerous variations have received thousands of papers over the past thirty years, in which a few hundred attractors were explored. These Chua's attractors were self-excited up until this point, though. The study of oscillations using some effective analytical and numerical approaches is the focus of the current survey. The current trends in the synthesis of analytical and numerical methods are attempting to be reflected in this.

3.2 Self-Excited Attractors

During the early stages of the foundation of the theory of nonlinear oscillations, which took place in the first half of the twentieth century, the analysis and synthesis of oscillating systems, in which the issue of the existence of oscillations could be resolved with relative ease, received a lot of attention. This approach was backed by the study of periodic oscillations in practical fields, including mechanics, electronics, chemistry, and biology.

Definition 3.2.1 *An attractor is called a self-excited attractor if its basin of attraction intersects with any open neighborhood of an unstable fixed point.*

Moreover, in the middle of the twentieth century, except for self-excited periodic oscillations in applied systems, chaotic oscillations were found numerically to be excited from an unstable equilibrium and could be computed by the standard computational procedure. Take a look at some traditional illustrations of self-excited oscillations.

Example 3.2.1 *Rayleigh [1877] was the first to demonstrate that in a two-dimensional nonlinear dynamical system undamped vibrations might emerge without external periodic action while researching string oscillations (limit cycles).[32]*

Consider the limit cycle localization in the Rayleigh system

$$\ddot{x} - (\alpha - \beta \dot{x}^2)\dot{x} + x = 0, \quad (3.1)$$

for $\alpha = 1$, $\beta = 0.1$. In figure (3.1), a two trajectories (each starting in red and ending in green) localize a limit cycle by drawing attention to it.

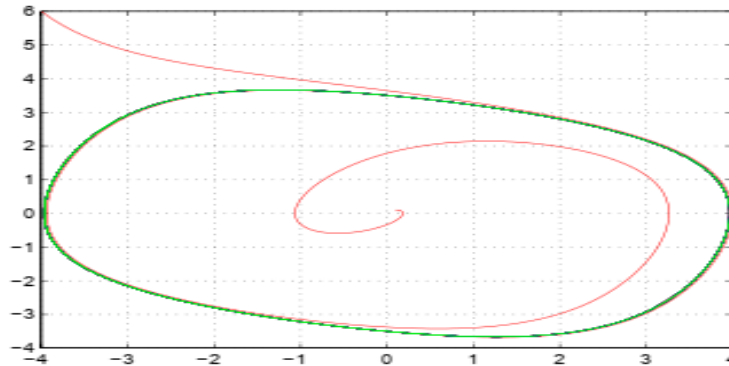


Figure 3.1: Localization of limit cycle in Rayleigh system

Example 3.2.2 Take into account electrical circuit oscillations, such as those produced by the van der Pol oscillator [van der Pol, 1926].[32]

$$\ddot{x} + a(x^2 - 1)\dot{x} + x = 0, \quad (3.2)$$

where the result was found for $a = 2$. (see figure (3.2))

3.3 Hidden Oscillations

David Hilbert was the first to evade the challenge of examining concealed oscillations [17]. In relation to the degree of the polynomials under consideration, he introduced the

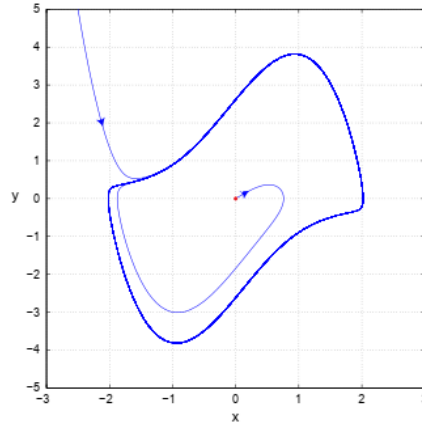


Figure 3.2: Numerical localization of limit cycle in van der Pol oscillator

problem of the investigation of the number and potential arrangements of limit cycles in two-dimensional polynomial systems in 1900.

According to the study, self-excited periodic and chaotic oscillations did not provide all of the information regarding the potential types of oscillations. The models of periodic and chaotic oscillations of different types were discovered in the middle of the 20th century. Because the basin of attraction was not cut away with small neighborhoods of equilibria, these models were dubbed "hidden oscillations" and "hidden attractors" in 2011 [30]. Therefore, the following definition should be supplied in order to allow for this class of attractor.

Definition 3.3.1 *If an attractor's basin of attraction is not cut off by small regions of equilibria (stable equilibria point), it is referred to as a "hidden attractor."*

The difficulty of numerical localization and analytical examination of hidden attractors has increased significantly in recent years. This occurs because using equilibrium information to organize identical passing processes according to the conventional computational approach is not possible in this situation. As a result, this common method cannot be used to compute the hidden attractors. Furthermore, since a basin of attraction can be so small and the hidden attractor's own dimension can be much smaller than the dimension

of the considered system, it is not possible in this situation for the integration of trajectories into random initial data to expand hidden attractor localization. Consider some good examples of hidden attractors.

Example 3.3.1 *In 1963, the Lorenz system was the first well-known example of a visualization of a chaotic attractor in a dynamical system, corresponding to the excitation of a chaotic attractor from unstable equilibria..[32]*

Consider Lorenz system

$$\begin{cases} \dot{x} = a(y - x), \\ \dot{y} = x(c - z) - y, \\ \dot{z} = xy - bz. \end{cases} \quad (3.3)$$

It's simulation with standard parameters is $a = 10$, $b = \frac{8}{3}$, $c = 28$. (see figure (3.3))

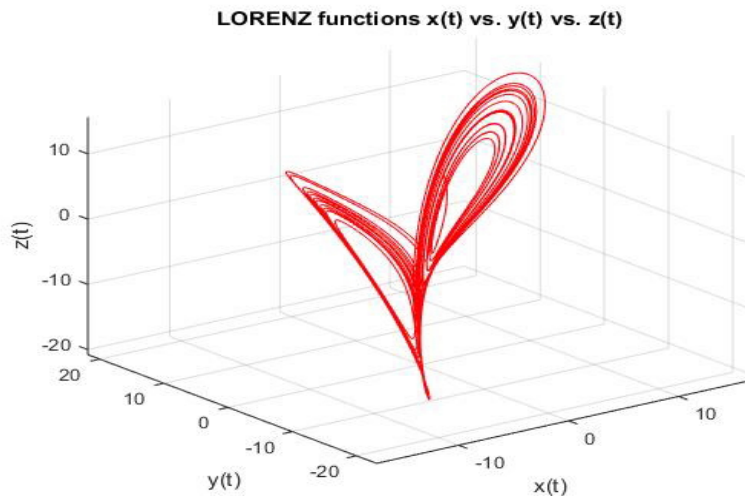


Figure 3.3: Numerical localization of chaotic attractor in Lorenz system

Example 3.3.2 *Consider the behavior of the classical Chua circuit [Chua, 1992]. In the*

dimensionless coordinates, a dynamic model of this circuit is as follows: [32]

$$\begin{cases} \dot{x} = a(y - x) - af(x), \\ \dot{y} = x - y + z, \\ \dot{z} = -(by + cz). \end{cases} \quad (3.4)$$

Here the function

$$f(x) = \alpha_1 x + \frac{1}{2}(\alpha_0 - \alpha_1)(|x + 1| - |x - 1|). \quad (3.5)$$

For simulation of this system, we use the following parameters: $a = 9.35$, $b = 14.79$, $c = 0.016$, $\alpha_0 = -1.1384$, $\alpha_1 = 0.7225$. (see figure (3.4))

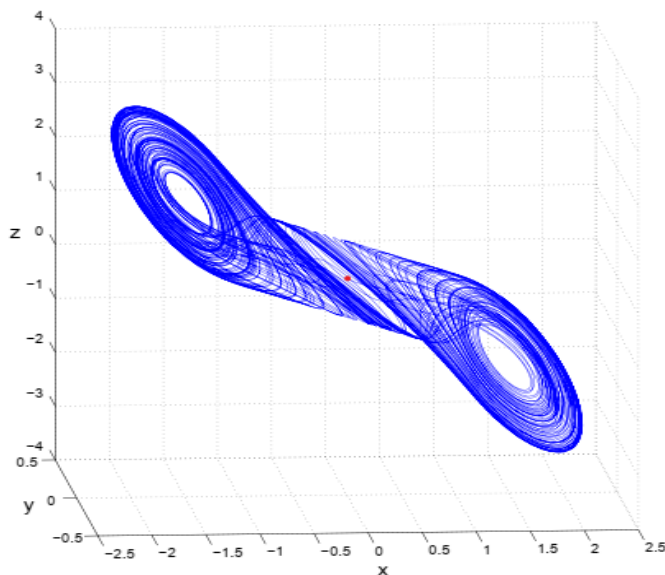


Figure 3.4: The numerical localization of chaotic attractor in Chua's circuit.

Remark 3.3.1 *The hidden vs. self-excited classification of attractors was introduced in connection with the discovery of the first hidden Chua attractor. [20]*

3.4 Analytical-Numerical Method for Hidden Attractor Localization

Recently, new concepts such as self-excited and concealed attractors have been introduced [28], [29] and [31]. If an attractor's basin of attraction crosses over with the area around an equilibrium point, it is referred to as a self-excited attractor; otherwise, it is referred to as a hidden attractor. For systems with no equilibria, only one stable equilibrium, or infinitely many stable equilibria, for instance, hidden attractors are attractors. It is particularly challenging to locate a hidden attractor since its basin of attraction does not overlap with any local communities of equilibrium points. This computational complexity is where the name "hidden" originates. Leonov et al., [27], [30], and [31] discovered a way to quantitatively prove their existence. They use this technique in particular for Chua attractors.

The approach

$$\frac{dX}{dt} = HX + \mu\Psi(\kappa^T X), \quad X \in \mathbb{R}^3, \quad (3.6)$$

where H is a constant $(n \times n)$ -matrix, μ, κ are constant n -dimensional vectors, T is a transposition operation, $\Psi(\sigma)$ is a continuous piecewise-differentiable scalar function, and $\Psi(0) = 0$. Define coefficient k' of harmonic linearization in such way that the matrix

$$H_0 = H + k' \mu \kappa^T, \quad (3.7)$$

has a pair of purely imaginary eigenvalues $\pm i\omega_0$ ($\omega_0 > 0$) and the rest of its eigenvalues have negative real parts. We assume that such k' exists. Rewrite system (3.6) as

$$\frac{dX}{dt} = H_0 X + \mu\varphi(\kappa^T X), \quad (3.8)$$

where $\varphi(\sigma) = \Psi(\sigma) - k'\sigma$, and introduce a finite sequence of functions $\varphi^0(\sigma), \varphi^1(\sigma), \dots, \varphi^m(\sigma)$

such that the graphs of neighboring function $\varphi^j(\sigma)$ and $\varphi^{j+1}(\sigma)$, ($j = 0, \dots, m - 1$), differ slightly from one another, where the function $\varphi^0(\sigma)$ is small, and $\varphi^m(\sigma) = \varphi(\sigma)$. Using a smallness of function, we can apply the method of harmonic linearization (describing function method) for the system

$$\frac{dX}{dt} = H_0 X + \varphi^0(\kappa^T X), \quad (3.9)$$

and determine a stable nontrivial periodic solution $X^0(t)$.

For the localization of attractor of original system(3.8), we will follow numerically the transformation of this periodic solution. All the points of this stable periodic solution are located in the domain of attraction of the stable periodic solution $X^1(t)$ of the system

$$\frac{dX}{dt} = H_0 X + \varphi^j(\kappa^T X), \quad (3.10)$$

With $j = 1$, or when passing from (3.9) to system (3.10) with $j = 1$, one can observe the instability bifurcation destroying the periodic solution. In the first case, it is possible to find $X^1(t)$ numerically, taking as initial condition of system (3.10) with $j = 1$, any point of the stable periodic solution $X^0(t)$. Starting from this initial condition, after a transient phase, the trajectory reaches the periodic solution $X^1(t)$. Then, after the computation of $X^1(t)$, it is possible to obtain a periodic trajectory $X^2(t)$ of system (3.10) with $j = 2$ starting from any point of the stable periodic solution $X^1(t)$, and so on, to obtain a periodic solution of system (3.8) if such solution exists.

Remark 3.4.1 *In some cases, it is not possible to get such a solution because one observes at a certain step an instability bifurcation destroying the periodic solution.*

Remark 3.4.2 *In the case of the Chua attractor, the periodic solution close to the harmonic one is transformed into a chaotic attractor. This is also the case for multispiral chaotic attractors from saturated function series, studied in this thesis.*

A linear nonsingular transformation S ($X = SY$) can transform system (3.9) to the form:

To determine the initial condition $X^0(0)$ of the periodic solution, a linear nonsingular transformation S ($X = SY$) can transform system (3.9) to the form:

$$\begin{cases} \dot{y}_1 = -\omega_0 y_2 + v_1 \varphi^0(y_1 + u_3^T Y_3), \\ \dot{y}_2 = \omega_0 y_1 + v_2 \varphi^0(y_1 + u_3^T Y_3), \\ \dot{Y}_3 = A_3 Y_3 + V_3 \varphi^0(y_1 + u_3^T Y_3). \end{cases} \quad (3.11)$$

Here y_1, y_2 are scalar values; Y_3 is an $(n - 2)$ –dimensional vector, V_3 et u_3 $(n - 2)$ –dimensional vector, v_1 and v_2 are real numbers; A_3 is an $(n - 2) \times (n - 2)$ matrix, where all of its eigenvalues have negative real parts. Without loss of generality, it can be assumed that for the matrix A_3 there exists a positive number $d_2 > 0$ such that

$$Y_3^t (A_3 + A_3^t) Y_3 \leq -2d_2 |Y_3|^2, \quad \forall Y_3 \in \mathbb{R}^{n-2}. \quad (3.12)$$

In the scalar case, let us introduce the describing function Φ of a real variable η :

$$\Phi(\eta) = \int_0^{2\pi/\omega_0} \varphi(\cos(\omega_0 t)\eta) \cos(\omega_0 t) dt. \quad (3.13)$$

Theorem 3.4.1 [57] *If a positive η_0 such that*

$$\Phi(\eta_0) = 0, \quad v_1 \frac{d\Phi(\eta)}{d\eta} \Big|_{\eta=\eta_0} < 0, \quad (3.14)$$

then for the initial condition of the periodic solution $X^0(0) = S(y_1(0), y_2(0), Y_3(0))^T$ at the first step of algorithm we have

$$y_1(0) = \eta_0 + O(\varepsilon), \quad y_2(0) = 0, \quad Y_3(0) = O_{n-2}(\varepsilon), \quad (3.15)$$

were $O_{n-2}(\epsilon)$ is an $(n - 2)$ -dimensional vector such that all its components are $O(\epsilon)$.

For the stability of $X^0(t)$ (where stability is defined in the sense that for all solutions with the initial data sufficiently close to $X^0(0)$ the modulus of their difference with $X^0(t)$ is uniformly bounded for all $t > 0$) it is sufficient to require the following condition is true $b_1 \frac{d\Phi(\eta)}{d\eta} |_{\eta=\eta_0} < 0$.

In practice, to determine k' and ω_0 one uses the transfer function $W(\lambda)$ of system (3.6) :

$$W(\lambda) = \kappa^T (H - \lambda I)^{-1} \mu, \quad (3.16)$$

where λ is a complex variable. The number ω_0 is determined from the equation $\text{Im } W(i\omega_0) = 0$ and k' is calculated then by the formula $k' = -\text{Re } W(i\omega_0)^{-1}$.

3.4.1 Example (Hidden Attractor for Chua's System)

In Chua's circuit, a hidden chaotic attractor was found for the first time in 2010 [Kuznetsov et al., 2011] [27]-[28], three-dimensional dynamical system's description. The application of the aforementioned approach to the localization of a hidden chaotic attractor in Chua's system will be shown below. The authors used the method above to discover a hidden attractor. For this purpose, write Chua's system (3.4-3.5) in the form (3.6)

$$\frac{dX}{dt} = HX + \mu\Psi(\kappa^T X), \quad X \in \mathbb{R}^3. \quad (3.17)$$

Here,

$$H = \begin{pmatrix} -a(\alpha_1 + 1) & a & 0 \\ 1 & -1 & 1 \\ 0 & -b & -c \end{pmatrix}, \quad \mu = \begin{pmatrix} -a \\ 0 \\ 0 \end{pmatrix}, \quad \kappa = \begin{pmatrix} 1 \\ 0 \\ 0 \end{pmatrix}$$

and $\Psi(\sigma) = \varphi(\sigma)$.

Introduce the coefficient k' and small parameter ε , and represent system (3.17) as

$$\frac{dX}{dt} = H_0 X + \mu \varepsilon \varphi(\kappa^T X), \quad (3.18)$$

where

$$H_0 = H + k' \mu \kappa^T = \begin{pmatrix} -a(\alpha_1 + 1 + k') & a & 0 \\ 1 & -1 & 1 \\ 0 & -b & -c \end{pmatrix}, \quad \lambda_{1,2}^{H_0} = \pm i\omega_0, \quad \lambda_3^{H_0} = -d,$$

By nonsingular linear transformation $X = ZY$ system (3.18) is compressed into the form

$$\frac{dy}{dt} = Py + v \varepsilon \varphi(u^T Y), \quad (3.19)$$

where

$$P = \begin{pmatrix} 0 & -\omega_0 & 0 \\ \omega_0 & 0 & 0 \\ 0 & 0 & -d \end{pmatrix}, \quad v = \begin{pmatrix} v_1 \\ v_2 \\ 1 \end{pmatrix}, \quad Y = \begin{pmatrix} y_1 \\ y_2 \\ Y_3 \end{pmatrix} \text{ and } u = \begin{pmatrix} 1 \\ 0 \\ -h \end{pmatrix}$$

The transfer function $W_P(\lambda)$ of system (3.19) can be represented as

$$W_P(\lambda) = \frac{-v_1 \lambda + v_2 \omega_0}{\lambda^2 + \omega_0^2} + \frac{h}{\lambda + d}.$$

Further, using the equality of transfer functions of systems (3.18) and (3.19), we obtain

$$W_P(\lambda) = \kappa^T (H_0 - \lambda I)^{-1} \mu.$$

This implies the relations indicated below:

$$\begin{aligned}
 k' &= \frac{-a(\alpha_1 + \alpha_1 c + c) + \omega_0^2 - c - b}{a(1+c)}, \\
 d &= \frac{a + \omega_0^2 - b + 1 + c + c^2}{1+c}, \\
 h &= \frac{a(c+b-(1+c)d+d^2)}{\omega_0^2 + d^2}, \\
 b_1 &= \frac{a(c+b-\omega^2-(1+c)d)}{\omega_0^2 + d^2}, \\
 b_2 &= \frac{a((c+b)d + (1+c-d)\omega_0^2)}{\omega_0(\omega_0^2 + d^2)}.
 \end{aligned} \tag{3.20}$$

Since system (3.18) can be reduced to the form (3.19) by the nonsingular linear transformation $X = ZY$, for the matrix S the following relations

$$P = Z^{-1}HZ, \quad b = Z^{-1}\mu, \quad c^T = \kappa^T S, \tag{3.21}$$

are true. The entries of this matrix are obtained by solving these matrix equations:

$$Z = \begin{pmatrix} Z_{11} & Z_{12} & Z_{13} \\ Z_{21} & Z_{22} & Z_{23} \\ Z_{31} & Z_{32} & Z_{33} \end{pmatrix}.$$

Here

$$\begin{aligned}
 Z_{11} &= 1, & Z_{12} &= 0, & Z_{13} &= -h, \\
 Z_{21} &= \alpha_1 + 1 + k', & Z_{22} &= \frac{-\omega_0}{a}, & Z_{23} &= -\frac{h(a(\alpha_1 + 1 + k') - d)}{a}, \\
 Z_{31} &= \frac{a(\alpha_1 + k') - \omega_0^2}{a}, & Z_{32} &= \frac{a(b+c)(\alpha_1 + k') + ab + -\omega_0^2}{a\omega_0}, \\
 Z_{33} &= h \frac{a(\alpha_1 + k')(d-1) + d(1+a-d)}{a}.
 \end{aligned}$$

We determine initial data for the first step of a multistage localization procedure for small

enough ε , as

$$X(0) = ZY(0) = S \begin{pmatrix} \eta_0 \\ 0 \\ 0 \end{pmatrix} = \begin{pmatrix} \eta_0 Z_{11} \\ \eta_0 Z_{21} \\ \eta_0 Z_{31} \end{pmatrix}. \quad (3.22)$$

The starting condition for the system (3.4-3.5) is provided by this.

$$X^0(0) = (x^0(0) = \eta_0, y^0(0) = \eta_0(1 + \alpha_1 + k'), z^0(0) = \eta_0 \frac{a(1 + \alpha_1) - \omega_0^2}{a}). \quad (3.23)$$

Consider system (3.18) with the parameters

$$a = 8.4562, b = 12.0732, c = 0.0052, \alpha_0 = -0.1768, \alpha_1 = -1.1468. \quad (3.24)$$

There are three equilibria in the system for the parameter values under consideration: a locally stable zero equilibrium and two saddle equilibria. Let's now employ the hidden attractor localization process described above to Chua's system (3.17) with parameters (3.24). Calculate a beginning frequency and a harmonic linearization coefficient for this.

$$\omega_0 = 2.0392, k' = 0.2098. \quad (3.25)$$

Then, we compute solutions of system (3.18) with the nonlinearity $\varepsilon(\Psi(x) - k'x)$ sequentially increasing ε from the value $\varepsilon_1 = 0.1$ to $\varepsilon_{10} = 1$ with step 0.1. By (3.20) and (3.23), the initial data can be obtained

$$x(0) = 9.4287, y(0) = 0.5945, z(0) = -13.4705,$$

for the initial phase of a multi-stage process. For $\varepsilon = 0.1$, the computation approaches the beginning oscillation $X^1(t)$ following a transitory process. Additionally, the set a hidden is calculated for the original Chua's system (3.17) using numerical methods and the

sequential transformation $X^j(t)$ with increasing parameter ε_j . In Fig.(3.5) , this collection is displayed.

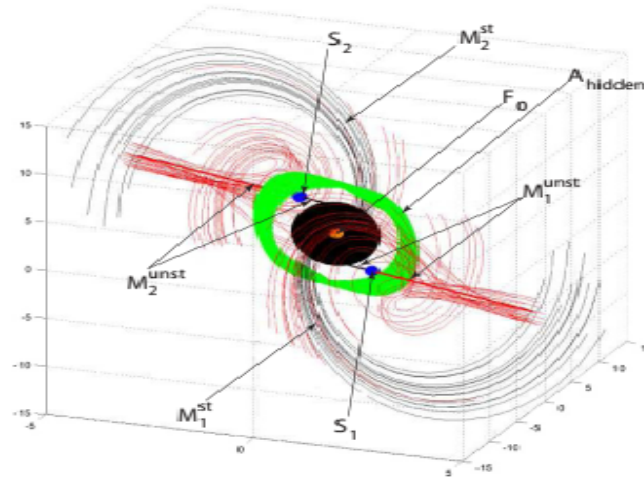


Figure 3.5: Hidden attractor localization

Chapter 4

Hidden Modalities of Spirals of Chaotic Attractor via Saturated Function Series and Numerical Results

4.1 Introduction

In 2016, Menacer et al. [39] discovered a number of hidden bifurcations in the multispiral Chua system using a different application of the Kuznetsov and Leonov technique presenting a sine function (T.Menacer 2016) [39]. Within the system (4.1-4.2) shown in [36], the two parameters p and q determine the number of spirals. according to the equation $N = p + q + 2$. It is because p and q are integers. It is impossible to continuously change it, making observation impossible. the attractors' bifurcation into m and $m + 2$ spirals when the parameters P and q shift. Additionally, non-integer real numbers cannot be used for p and q .

When we fix p and q and introduce the new control parameter ε the nonlinear part,

in order to discover the hidden bifurcations, governed by a homotopy parameter ε while keeping p and q constant. This element when fluctuates between 0 and 1, when ε takes a value of 0 for the non-linear component of system (4.1-4.2) is unpaired, and a cycle-shaped attractor is produced. However, if ε equal to 1, we discover the original system's attractor (4.1-4.2), with spirals, where $m = p + q + 2$. The number of spirals increases in direct proportion to the difference between these two values of ε . For each value discovered the new parameter, a technique is used during the integration operation to have odd or prior to locating the asymptotical attractor, for even numbers of spirals, the number of spirals grows incrementally until it reaches the maximum number that matches. The value guaranteed by ε the unveiling of the modalities of an odd number spirals

4.2 1-D n-Scroll Chaotic Attractors From Saturated Function Series

Among the various techniques for producing n -spiral ($n \geq 3$) chaotic attractors [49]-[57], for the one in [36], which is based on saturated function series (Fig. (4.1)) a controller is added to a linear system

$$\begin{cases} \dot{x} = y, \\ \dot{y} = z, \\ \dot{z} = -\alpha x - \beta y - \gamma z + r_1 f(x; k; h; p; q), \end{cases} \quad (4.1)$$

where

$$f(x; k; h; p; q) = \begin{cases} y_{1,k} & \text{if } x > qh + 1, \\ y_{2,k,i} & \text{if } |x - ih| \leq 1, -p \leq i \leq q, \\ y_{3,k,i} & \text{if } l_{1,i} < x < l_{2,i} \text{ and } -p < i < q - 1, \\ y_{4,k} & \text{if } x < -qph - 1, \end{cases} \quad (4.2)$$

with

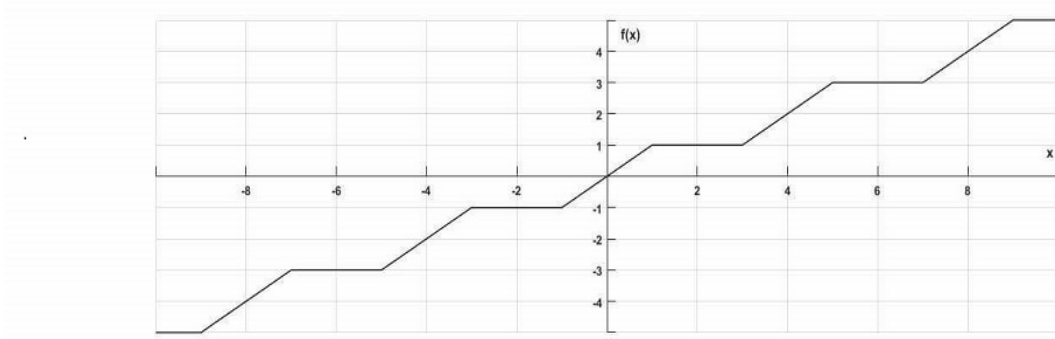


Figure 4.1: Saturated function series with $k = 9, h = 18, p = 2, q = 2$

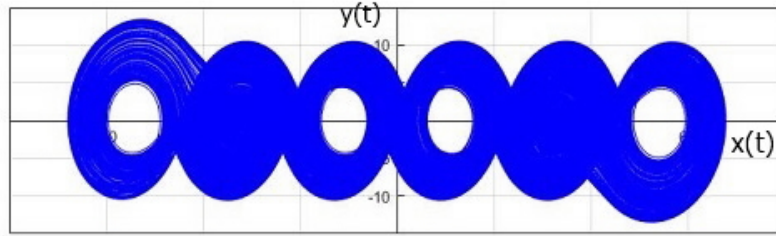


Figure 4.2: The 6-spiral attractor generated by Eqs.(4.1)and (4.2) with $k=9, h=18, p=q=2$ and $a=b=c=d_1=0,7$

$l_{1,i} = ih + 1$ and $l_{2,i} = (i + 1) * h - 1, y_{1,k} = (2q + 1) k, y_{2,k,i} = k (x - ih), y_{3,k,i} = (2i + 1) k$ and $y_{4,k} = -(2p + 1)k$.

Parameters p, q, h and k are integers, and $\alpha, \beta, \gamma, r_1$ are real numbers.

Throughout this study, set the parameter values as $\alpha = \beta = \gamma = r_1 = 0.7$. The number m of spirals.

$$m = p + q + 2 \tag{4.3}$$

For $k = 9, h = 18, p = q = 2$, a 6-spirals attractor is generated as the asymptotic attractor of system (4.1-4.2), see Fig. (4.2).

*** Attraction Basin of the 6 Spirals Attractors**

For our system (4.1-4.2) we have a $2(p + q) + 3$ equilibrium point are situated along

the x -axis, and fall into two different categories.

$$R_x = \left\{ -\frac{(2p+1)r_1k}{\alpha}, \frac{(-2p+1)r_1k}{\alpha}, \dots, \frac{(2q+1)r_1k}{\alpha} \right\}$$

$$S_x = \left\{ -\frac{pkr_1(h-2)}{kr_1-\alpha}, \frac{-(p+1)kr_1(h-2)}{kr_1-\alpha}, \dots, \frac{qkr_1(h-2)}{kr_1-\alpha} \right\}$$

For all equilibria in tow sets R_x and S_x are unstable points (saddle points) (for more information see [36]).

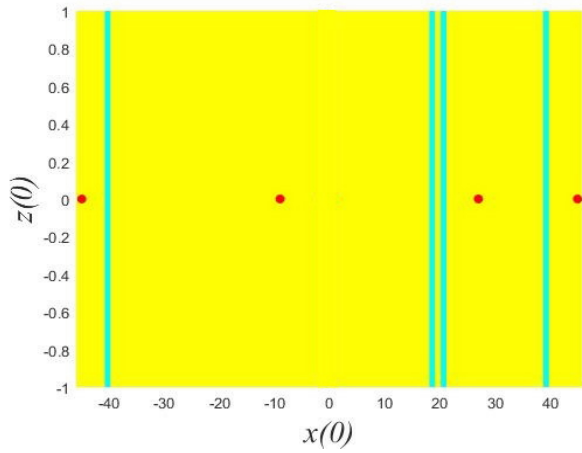
When we took $p = q = 2$ so we have a 11 equilibrium points

$$(-45; 0; 0), (-27; 0; 0), (-9; 0; 0), (0; 0; 0), (27; 0; 0),$$

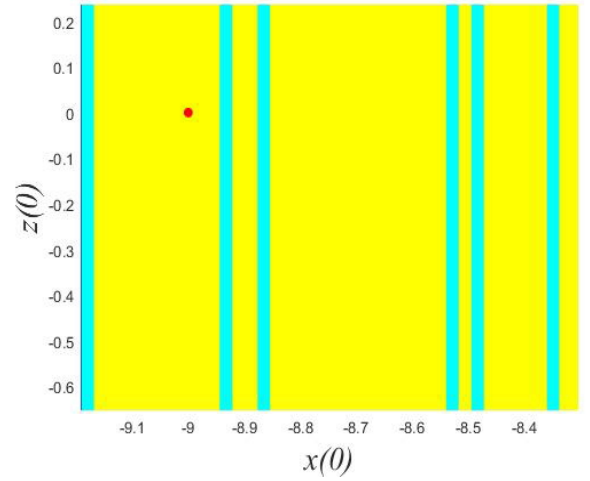
$$(45; 0; 0), (74 : 667; 0; 0), (149; 334; 0; 0), (224; 0001; 0; 0)$$

(three double points), are saddle points.

If the attraction in the chaotic attractors' basin does not cross paths with the unbounded neighborhood of equilibrium points, the chaotic attractors are known as hidden attractors. Since all of the points in our system are unstable, we haven't hidden attractors, thus the attraction basin is what we're interested in. We took six points because we saw that the same outcomes appeared in all the figures. The yellow region represents the chaotic attractors' attraction basin, while the cyan region shows the motion that starts in these initial state regions and will diverge from equilibrium points. This is seen in figures below:

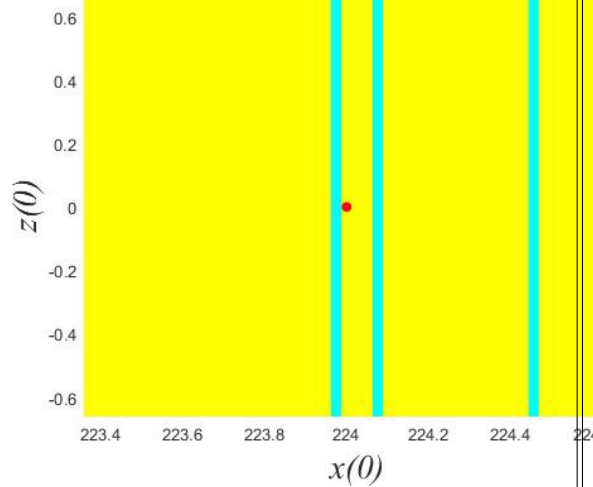


Attraction basin of 6 spirals attractors cross section passing through four equilibrium points $(45,0,0)$; $(-45,0,0)$, $(-9, 0,0)$, $(27,0,0)$.

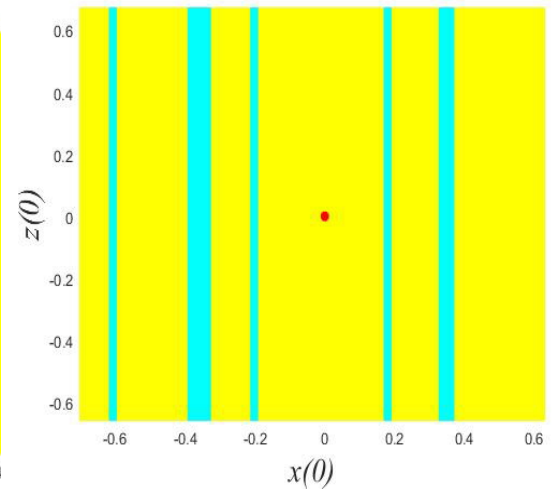


Attraction basin zooming in around $(-9,0,0)$ equilibrium point

1000)



27.jpg
Attraction basin zooming in around $(224.0001,0,0)$ equilibrium point



Attraction basin zooming in around $(0; 0; 0)$ equilibrium point

4.3 Recovering Hidden Bifurcation in a Multispiral Chaotic Attractor

To prove this obstacle, Menacer et al. [39] presented a novel procedure for uncovering hidden bifurcations based on the idea of Leonov and Kuznetsov [27] for investigating hidden attractors (i.e. homotopy and numerical continuation, see chapter 2. This procedure is novelly applied to multi-scroll chaotic attractors from saturated function series. We recall this procedure in this section in which the values of parameters are fixed at $a = b = c = d_1 = 0.7, k = 9, h = 18$.

Rewrite system (4.1-4.2) to the form

$$\frac{dX}{dt} = HX + \mu\Psi(\kappa^T X), \quad X \in \mathbb{R}^3. \quad (4.4)$$

Here

$$H = \begin{pmatrix} 0 & 1 & 0 \\ 0 & 0 & 1 \\ -\alpha & -\beta & -\gamma \end{pmatrix}, \quad \mu = \begin{pmatrix} 0 \\ 0 \\ r_1 \end{pmatrix}, \quad \kappa = \begin{pmatrix} 1 \\ 0 \\ 0 \end{pmatrix},$$

and $\Psi(\sigma) = \varphi(\sigma)$.

Introduce the coefficient k' and small parameter ε , and represent system (4.4) as

$$\frac{dX}{dt} = H_0 X + \mu\varepsilon\varphi(\kappa^T X), \quad (4.5)$$

where

$$H_0 = H + k' \mu \kappa^T = \begin{pmatrix} 0 & 1 & 0 \\ 0 & 0 & 1 \\ k' d_1 - \alpha & -\beta & -\gamma \end{pmatrix}, \quad \lambda_{1,2}^{H_0} = \pm i\omega_0, \quad \lambda_3^{H_0} = -d,$$

By nonsingular linear transformation $X = ZY$ system (4.5) is compressed into the form

$$\frac{dy}{dt} = Py + v\varepsilon\varphi(c^TY), \quad (4.6)$$

where

$$A = \begin{pmatrix} 0 & -\omega_0 & 0 \\ \omega_0 & 0 & 0 \\ 0 & 0 & -d \end{pmatrix}, \quad v = \begin{pmatrix} v_1 \\ v_2 \\ 1 \end{pmatrix}, \quad Y = \begin{pmatrix} y_1 \\ y_2 \\ Y_3 \end{pmatrix} \text{ and } c = \begin{pmatrix} 1 \\ 0 \\ -h \end{pmatrix}.$$

The transfer function $W_P(\lambda)$ of system (4.6) can be represented as

$$W_P(\lambda) = \frac{-v_1\lambda + v_2\omega_0}{\lambda^2 + \omega_0^2} + \frac{h}{\lambda + d}.$$

Further, using the equality of transfer functions of systems (4.5) and (4.6), we obtain

$$W_P(\lambda) = \kappa^T(H_0 - \lambda I)^{-1}\mu.$$

This indicates the relationships listed below :

$$\begin{aligned} k' &= \frac{\alpha - \omega_0^2 d}{r_1}, \\ d &= \gamma, \\ h &= \frac{-r_1}{\omega_0^2 + d^2}, \\ v_1 &= \frac{-r_1}{\omega_0^2 + d^2}, \\ v_2 &= \frac{-\gamma\omega_0^2}{\omega_0(\omega_0^2 + d^2)}. \end{aligned} \quad (4.7)$$

Since system (4.5) can be reduced to the form (4.6) by the nonsingular linear transformation $X = ZY$, for the matrix Z the following relations

$$P = Z^{-1}HZ, \quad v = Z^{-1}\mu, \quad c^T = \kappa^T Z, \quad (4.8)$$

are true. The entries of this matrix are obtained by solving these matrix equations:

$$Z = \begin{pmatrix} Z_{11} & Z_{12} & Z_{13} \\ Z_{21} & Z_{22} & Z_{23} \\ Z_{31} & Z_{32} & Z_{33} \end{pmatrix}.$$

Here

$$\begin{aligned} Z_{11} &= 1, & Z_{12} &= 0, & Z_{13} &= h, \\ Z_{21} &= 0, & Z_{22} &= -\omega_0, & Z_{23} &= dh, \\ Z_{31} &= -\omega_0^3, & Z_{32} &= 0, & Z_{33} &= d^2h. \end{aligned}$$

For small enough ε we determine initial data for the first step of multistage localization procedure, as

$$X(0) = ZY(0) = S \begin{pmatrix} \eta_0 \\ 0 \\ 0 \end{pmatrix} = \begin{pmatrix} \eta_0 Z_{11} \\ \eta_0 Z_{21} \\ \eta_0 Z_{31} \end{pmatrix}. \quad (4.9)$$

The starting condition for the system (4.4) is provided by this.

$$X^0(0) = (x^0(0) = \eta_0, y^0(0) = 0, z^0(0) = -\eta_0\omega_0^3). \quad (4.10)$$

4.3.1 Numerical Results of Hidden Bifurcations

One acquisition is required for the value of the parameters defined in this study : $k' = 0.3$, $d = 0.7$, $h' = -0.5882$, $v_1 = -0.5882$, $v_2 = -0.4901$, so this is the matrix Z

$$Z = \begin{pmatrix} 1 & 0 & 0.5882 \\ 0 & -0.84 & -0.41174 \\ -0.5927 & 0 & -0.2882 \end{pmatrix}.$$

Via theorem (3.4.1), for small enough ε we computed initial data for the first step of the multistage localization procedure.

$$X(0) = ZY(0) = Z \begin{pmatrix} \eta_0 \\ 0 \\ 0 \end{pmatrix} = \begin{pmatrix} \eta_0 Z_{11} \\ \eta_0 Z_{21} \\ \eta_0 Z_{31} \end{pmatrix}. \quad (4.11)$$

This provides the system's (3.6) starting data.

$$X^0(0) = x^0(0) = \eta_0, \quad y^0(0) = 0, \quad z^0(0) = -\eta_0 \omega_0^3. \quad (4.12)$$

We now put the above-described localization process to use on the system (4.1-4.2) with multiple spiral attractors. In order to do this, we compute the initial frequency shown below ω_0 and a coefficient of harmonic linearization:

$$\omega_0 = 0.84, \quad k' = 0.3. \quad (4.13)$$

Then, starting with step 0.4, we calculate the solutions of system 4.5 with the non-linearity $\varepsilon\varphi(x) = \varepsilon(\psi(x) - k_1x)$ by increasing ε sequentially from $\varepsilon = 0.4$ to $\varepsilon = 1$. If the stable periodic solution $X^1(t)$ corresponding to the small value $\varepsilon = 0.4$ is also close the harmonic one then, the solution $X^2(t)$ can be calculated numerically by seeking one trajectory of system (3.6) with $\varepsilon = 0.4$ picking as initial point $X^1(t_{max})$ where t_{max} is the recent value of the integration time. We survive by increasing the parameter ε and using the same numerical procedure to calculate $X^3(t), X^4(t), X^5(t), \dots, X^i(t) \dots$, which are system (4.1-4.2) solutions for specific initial data. We obtain detailed data for the solutions for increasing values of ε as shown in the tow tables (4.1-4.2).

So, from the tow tables (4.1-4.2), we obtain the solutions $X^1(0)$ with one spiral to $X^4(0)$ (see figures (4.3-4.4)). In each figure, there is a variant even number of spirals in the

Table 4.1: : Initial data according to the values of epsilon for 6 spirals

Values of ε	$X^i(0)$	x_0	y_0	z_0
0.4	$X^1(0) = X^0(t_{\max})$	-0.8	0	0.4742
0.6	$X^2(0) = X^1(t_{\max})$	-1.6412	-0.8137	-2.4791
0.95	$X^3(0) = X^2(t_{\max})$	-11.8094	2.6215	4.3874
0.98	$X^4(0) = X^3(t_{\max})$	14.1195	2.3715	-4.0961
0.99	$X^5(0) = X^4(t_{\max})$	20.597	-2.8517	4.9190
1	$X^6(0) = X^5(t_{\max})$	-0.5411	-0.2490	-6.2018

Table 4.2: : Initial data according to the values of epsilon for 4 spirals

Values of ε	$X^i(0)$	x_0	y_0	z_0
0.4	$X^1(0) = X^0(t_{\max})$	-1.78	0	1.253
0.6	$X^2(0) = X^1(t_{\max})$	-0.6904	0.5262	-2.6066
0.95	$X^3(0) = X^2(t_{\max})$	4.8838	-3.3862	0.6216
0.98	$X^4(0) = X^3(t_{\max})$	18.5373	-0.3588	-1.7539
1	$X^5(0) = X^4(t_{\max})$	-11.2090	-4.0556	1.1964

attractor. The number of spirals increases by two at each step, as shown on table (4.3) from 1 to 6 spirals (respectively 4 spirals see the table (4.4) and figure (4.3-4.4). The values of ε these two tables contain all of the bifurcation values.

Table 4.3: : Values of the parameter epsilon at the bifurcation points for $p = q = 2$

Values of ε	0.4	0.6	0.95	0.98	0.99	1
Number of spirals	1	2	4	6	6	6

Table 4.4: : Values of the parameter epsilon at the bifurcation points for $p = q = 2$

Values of ε	0.4	0.6	0.95	0.98	1
Number of spirals	1	2	4	4	4

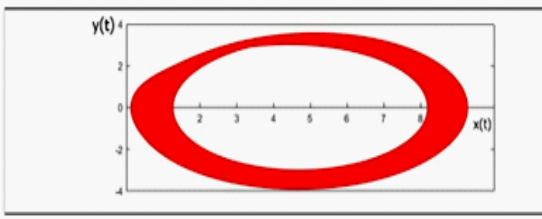


Fig. 6 1 spiral for $\varepsilon=0.4$

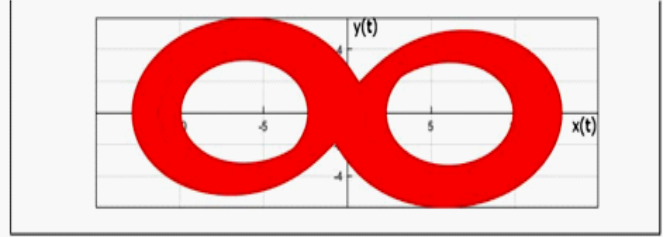


Fig. 7 2 spirals for $\varepsilon=0.6$

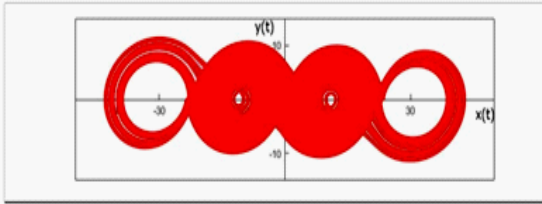


Fig. 8 4 spirals for $\varepsilon=0.95$

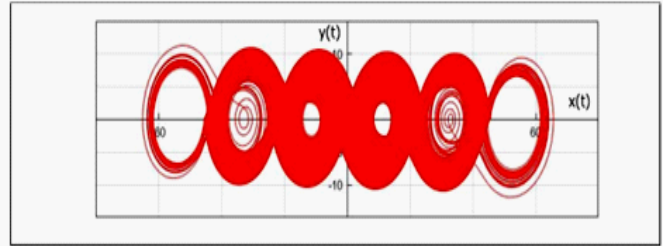


Fig. 9 6 spirals for $\varepsilon=0.98$

Figure 4.3: The bifurcation points for $p = q = 2$

4.3.2 The Influence of the Integration Duration Procedure for Unveiling Hidden Modalities of Odd Number of Spirals

We previously recalled in **section 4** that the hidden bifurcation track's attractors process an even number of spirals. The hidden modalities of an odd number of spirals are revealed using a novel technique that we describe in this section. The system (4.1-4.2) integration time serves as the foundation for this methodology. Through the use of this new method we have fixed ε and replicated the integration time t_{max} . Before reaching the even number of spirals asymptotical attractor, which is accessible during the integration process. As soon as the number of spirals has multiplied to the highest number that satisfies the value set by ε , we stop.

To study the effect of this integration duration on the base of this procedure, we repeat

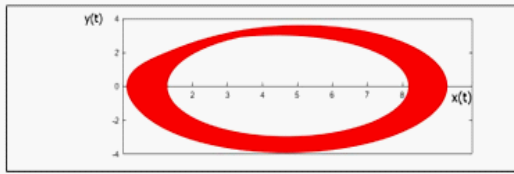


Fig. 10 1 spiral for $\varepsilon=0.4$

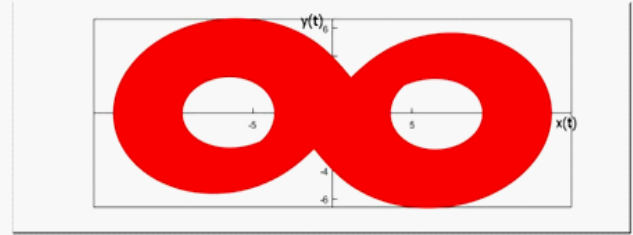


Fig. 11 2 spirals for $\varepsilon=0.6$

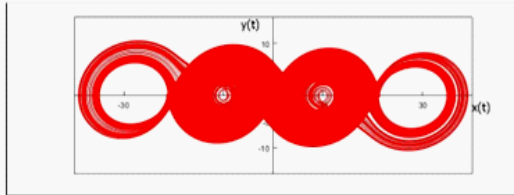


Fig. 12 4 spirals for $\varepsilon=0.95$

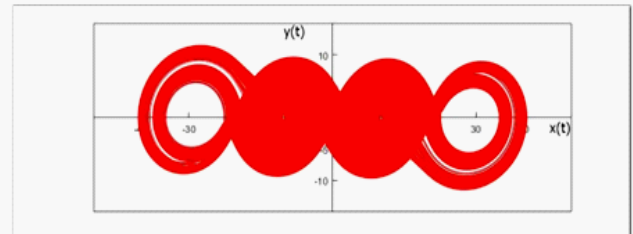


Fig. 13 4 spirals for $\varepsilon=0.98$

Figure 4.4: The bifurcation points for $p = q = 1$

the same procedure for all values of table (4.1), we are notice the change of spiral number and we summarize our results in table (4.3.2) and figures (numerical example 6 and 4 spirals) (4.5-4.6-4.7-4.8-4.9-4.10)

$\varepsilon = 0.4$	$t_{stepmax}$	500000				
	Nb of spirals	1				
$\varepsilon = 0.6$	$t_{stepmax}$	380	20000			
	Nb of spirals	1	2			
$\varepsilon = 0.95$	$t_{stepmax}$	200	1000	10000	50000	
	Nb of spirals	1	2	3	4	
$\varepsilon = 0.98$	$t_{stepmax}$	200	1000	2000	10000	40000
	Nb of spirals	1	2	3	4	5
	$t_{stepmax}$	100000				
$\varepsilon = 0.99$	Nb of spirals	6				
	$t_{stepmax}$	120	500	1000	3000	10000
	Nb of spirals	1	2	3	4	5
	$t_{stepmax}$	200000				
$\varepsilon = 1$	Nb of spirals	6				
	$t_{stepmax}$	130	1000	1145	1500	10000
	Nb of spirals	1	2	3	4	5
	$t_{stepmax}$	90000				
	Nb of spirals	6				

Table 3. Values of $t_{stepmax}$ for $\varepsilon = 0.4$ to $\varepsilon = 1$ and $m=6$.

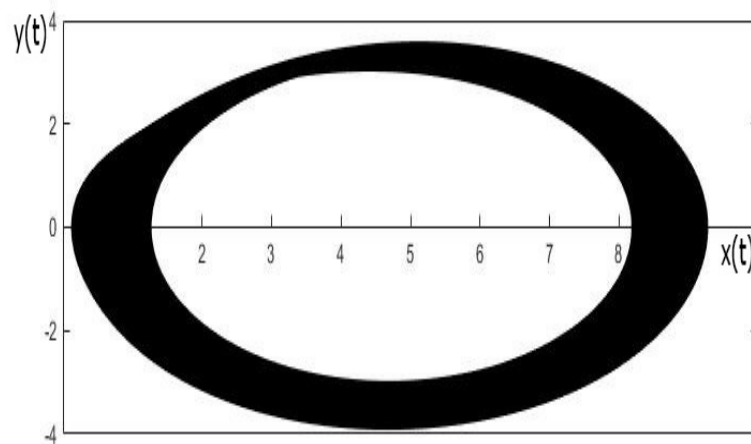


Figure 4.5: 1 spiral for $\varepsilon = 0.4$

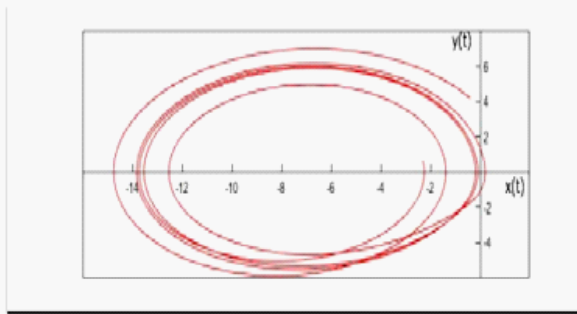


Fig. 16 1 spiral for $t_{stepmax} = 380$

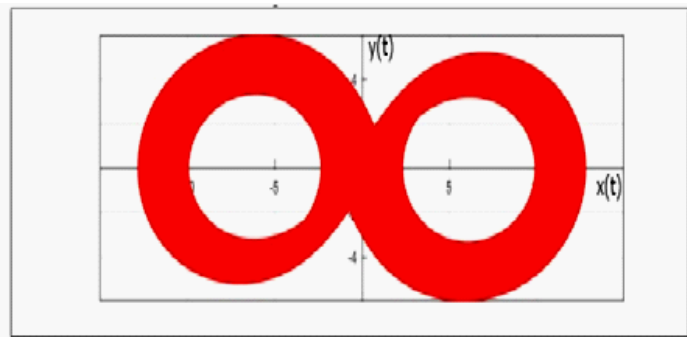


Fig. 17 2 spirals for $t_{stepmax} = 20000$

Figure 4.6: The increasing number of spirals for $\varepsilon = 0.6$ and various values of $t_{stepmax}$

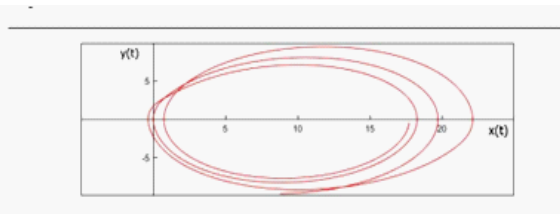


Fig. 19 1 spiral for $t_{stepmax} = 200$

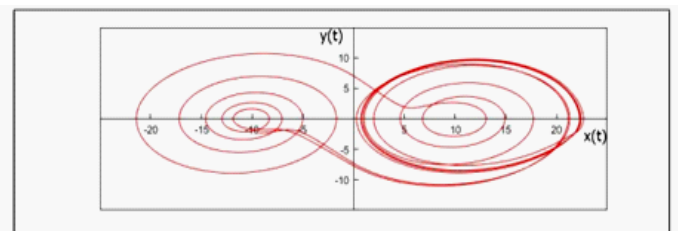


Fig. 20 2 spirals for $t_{stepmax} = 1000$

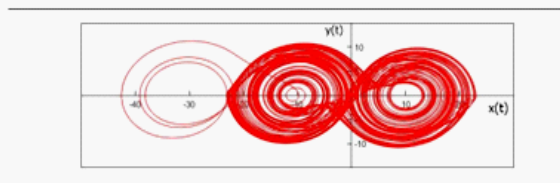


Fig. 21 3 spirals for $t_{stepmax} = 10000$

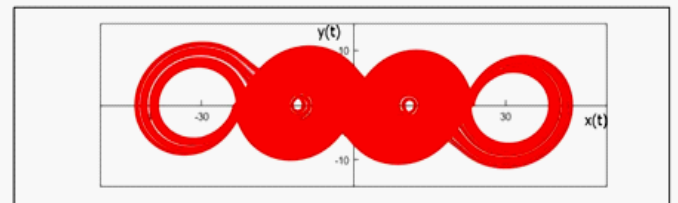


Fig. 22 4 spirals for $t_{stepmax} = 50000$

Figure 4.7: The increasing number of spirals for $\varepsilon = 0.95$ and various values of $t_{stepmax}$

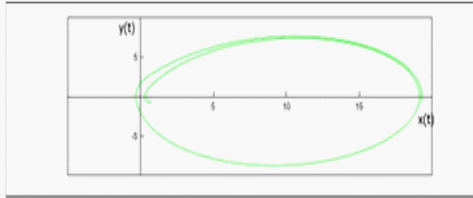


Fig. 24 1 spiral for $t_{stepmax} = 200$

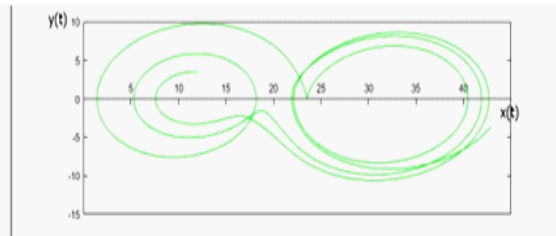


Fig. 25 2 spirals for $t_{stepmax} = 1000$

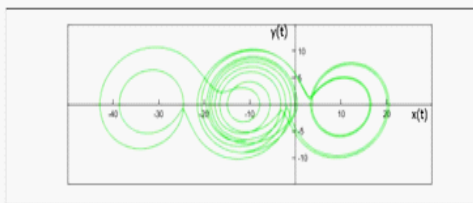


Fig. 26 3 spirals for $t_{stepmax} = 2000$

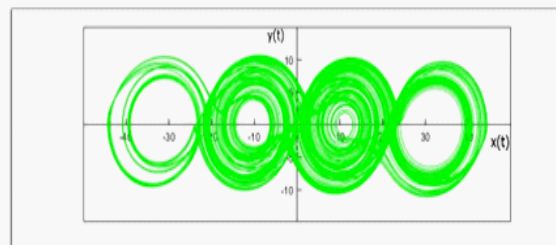


Fig. 27 4 spirals for $t_{stepmax} = 10000$

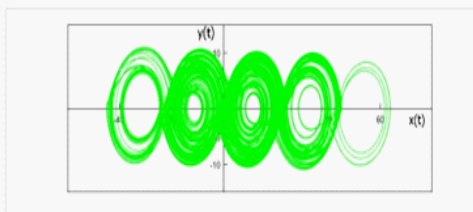


Fig. 28 5 spirals for $t_{stepmax} = 40000$

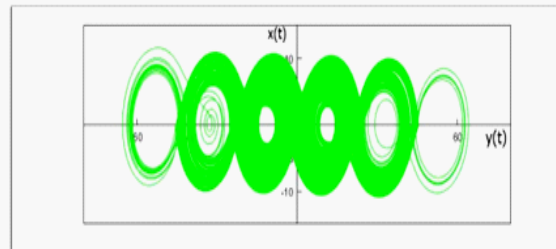


Fig. 29 6 spirals for $t_{stepmax} = 100000$

Figure 4.8: The increasing number of spirals for $\varepsilon = 0.98$ and various values of $t_{stepmax}$

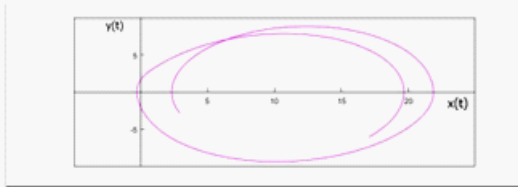


Fig. 31 1 spiral for $t_{stepmax} = 120$

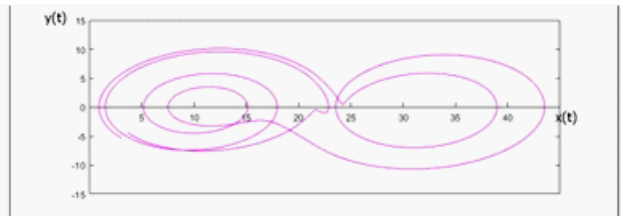


Fig. 32 2 spirals for $t_{stepmax} = 500$

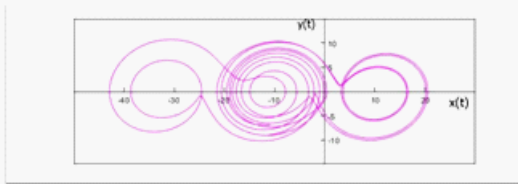


Fig. 33 3 spirals for $t_{stepmax} = 1000$

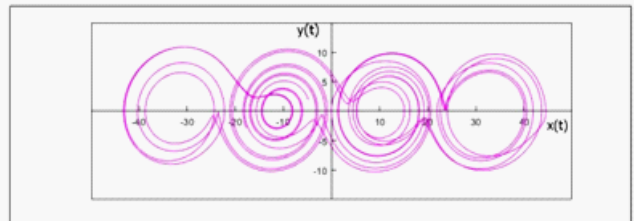


Fig. 34 4 spirals for $t_{stepmax} = 3000$

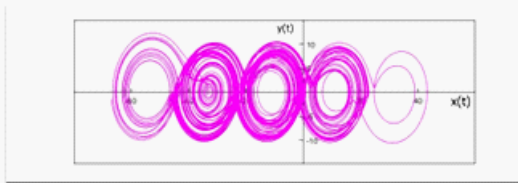


Fig. 35 5 spirals for $t_{stepmax} = 10000$

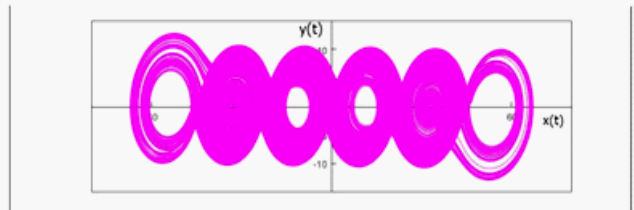


Fig. 36 6 spirals for $t_{stepmax} = 200000$

Figure 4.9: The increasing number of spirals for $\varepsilon = 0.99$ and various values of $t_{stepmax}$

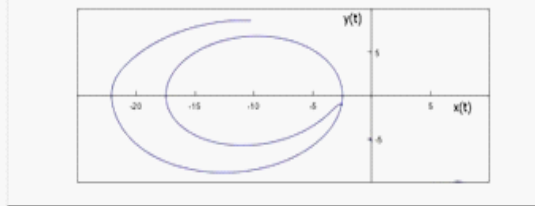


Fig. 38 1 spiral for $t_{stepmax} = 130$

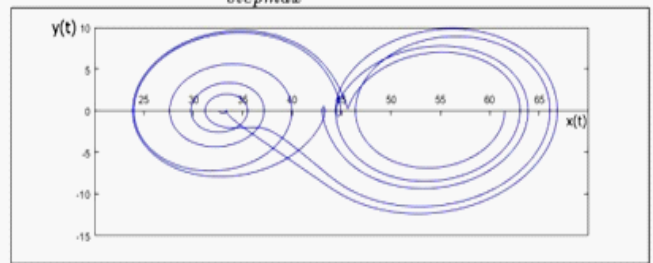


Fig. 39 2 spirals for $t_{stepmax} = 1000$

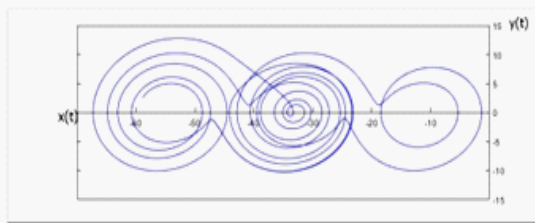


Fig. 40 3 spirals for $t_{stepmax} = 1145$

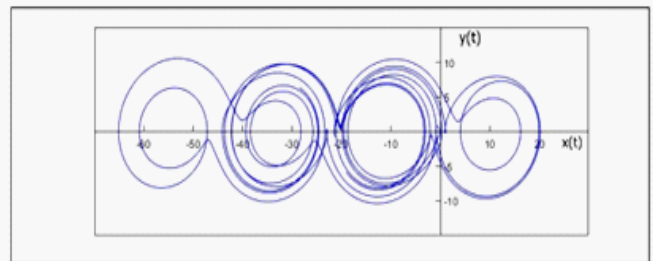


Fig. 41 4 spirals for $t_{stepmax} = 1500$

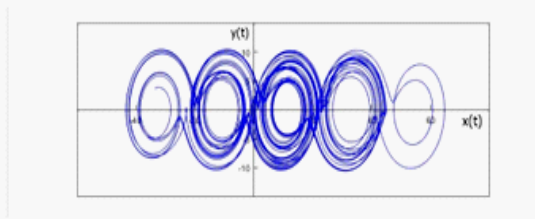


Fig. 42 5 spirals for $t_{stepmax} = 10000$

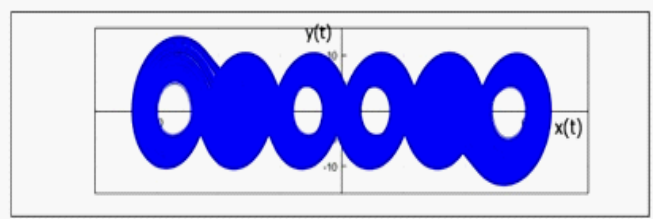


Fig. 43 6 spirals for $t_{stepmax} = 90000$

Figure 4.10: The increasing number of spirals for $\varepsilon = 1$ and various values of $t_{stepmax}$

Chapter 5

Symmetries in Hidden Bifurcation Routes to Multiscroll Chaotic Attractors Generated by Saturated Function Series

5.1 Introduction

Due to its potential uses in numerous real-world technologies, the production of multi-spiral chaotic attractors has received a great deal of attention over the last three decades. For a survey, see [35]. Several techniques have been proposed for creating multidirectional and multi-spiral chaotic attractors, including piecewise linear functions, nonlinear modulating functions, and electronic circuits (step, hysteresis, and saturation circuits). Even though the bulk of these multi-spiral generations have been known for a long time, bifurcation theory ([35]-[39]) has only lately been used to study them. The number of spirals (or scrolls) for any known multiscroll is a fixed integer that depends on one or more discrete characteristics. No bifurcation has been studied thus far. Menacer et

al. [39] introduced hidden bifurcations, yielding multispirals in a family of systems (4.6) with a continuous bifurcation parameter, changing the paradigm of discrete parameters.

The study of multispirals can thus be conducted using all the established theories of dynamical

systems and associated potent analytical techniques. The hidden attractor

theory developed by Leonov et al. ([27]-[28]) serves as the foundation for this hidden bifurcation theory.

The investigation of hidden bifurcation paths in $1 - D$ multi scroll chaotic attractors produced by saturated function series is the main topic of this chapter. This chapter investigates multi-spiral chaotic attractors produced by saturated function series via concealed bifurcation paths. The approach used by Menacer et al. (2016) [39] for Chua multi-spiral attractors to locate such hidden bifurcation routes (*HBR*) depends on two parameters.

These *HBR* are distinguished by coding the sequence in which the spirals emerge under the supervision of the two parameters and the maximum range extension of their attractors. These *HBR* also exhibit intriguing symmetries with relation to the two parameters.

5.2 Models and Properties of Bifurcation Routes

5.2.1 Numerical Calculation of Two hidden Bifurcations Routes

This chapter aims to investigate the hidden bifurcation paths and symmetries of the $1 - D$ multispiral attractors proposed in chapter 3. First, two instances of these covert bifurcation pathways are demonstrated, and the appearance of the spirals is made clear.

Consider the system (4.1-4.2) with parameter values

$$\alpha = \beta = \gamma = r_1 = 0,7.$$

Now, the localization procedure described above is applied to system (4.1) with multiple spiral attractors. For this purpose, the following starting frequency ω_0 and a coefficient of harmonic linearization k' are computed, as explained in the chapter 3 :

$$\omega_0 = 0.8366, \quad k' = 0.3.$$

Then, the solutions of system (4.5), with the nonlinearity $\varepsilon\varphi(x) = \varepsilon(\Psi(x) - k'x)$ are computed by increasing sequentially from the value $\varepsilon = 0.1$ to $\varepsilon = 1$, with step 0.1. For $p = 0$, $q = 4$, $h = 20$ and $k = 10$, using (4.10), one obtains the initial conditions

$$x_0(0) = 203.2, \quad y_0(0) = 0, \quad z_0(0) = -119.01,$$

whereas in the case of $p = 2$ and $q = 3$, with the same values of h and k the following initial conditions are obtained :

$$x_0(0) = 249, \quad y_0(0) = 0, \quad z_0(0) = -145.83.$$

The method outlined in section 3 produces the values of the parameter at the points of bifurcation, where the attractor increases the number of spirals from 1 to 6 spirals (7 spirals, respectively), as shown in tables 5.1 and 5.2. Be aware that instance 7 differs from case 6 in that the bifurcations appear in the following order 1, 2, 4, 6, and 7, respectively depending on the values of ε , as indicated in the images 5.2-5.3-5.4-5.5.

Table 5.1: : Values of the parameter epsilon at the bifurcation points for p = 0 and q = 4 (6 scrolls)

Values of ε	0.41	0.6
Number of spirals	1 spiral	2 spirals
Values of ε	0.95	0.985
Number of spirals	3 spirals	4 spirals
Values of ε	0.988	0.99
Number of spirals	5 spirals	6 spirals

Table 5.2: : Values of the parameter epsilon at the bifurcation points for $p = 2$ and $q = 3$ (7 scrolls)

Values of ε	0.42	0.6
Number of spirals	1 spiral	2 spirals
Values of ε	0.95	0.98
Number of spirals	4 spirals	6 spirals
Values of ε	0.99	
Number of spirals	7 spirals	

5.2.2 Maximal Attractor Range Extension and Coding Order of Spirals Appearance

Both tables (5.1) and (5.2) summarize the appearance of spirals versus the values of ε . Figs. 5.2 to 5.5 display some interesting information: the order of spiral appearance and the maximal attractor range extension. In both routes, the parameter values of function (4.2) are $k = 10$ and $h = 20$. These parameters play a significant role in the sizes of the attractors. The maximal attractor range extension ($MARE_{p,q}$) is the size of the x -projection of the considered attractor defined by parameter values p and q , when $\varepsilon = 1$ and as $t \rightarrow +\infty$. For example, for the first route defined in (5.1), one can see from fig 5.4 that the minimum value of the range of the variable x of the attractor is -20 , and the maximum value is 100 . Therefore, in this case, $MARE_{0,4} = [-20, 100]$, and its length is equal to 120 for 6 scrolls. For the second route in (5.2), the attractor spans between -60 and 80 (5.5) having $MARE_{2,3} = [-60, 80]$ with a length equal to 140 for 7 scrolls. In both cases, the length of $MARE$ is equal to the number of scrolls $\times 20$ (i.e. $(q+p+2) \times 20$, following (3)).

Moreover, when ε increases (figs 5.2 and 5.3), the size of each spiral is expanding. It is approximatively equal to $(17 \times \varepsilon) + 3$. By defining the interval $[v \times 20, w \times 20]^{\{\varepsilon\}}$ as

$$[v \times 20, w \times 20]^{\{\varepsilon\}} = [v \times (17 \times \varepsilon + 3), w \times (17 \times \varepsilon + 3)] \quad (5.1)$$

The initial spiral accomplishes the interval. $[0, 20]^{\{\varepsilon\}}$. The second scroll accomplishes the interval and is symmetrical to the first. $[-20, 20]^{\{\varepsilon\}}$. Now, introduce the coding $[0, 20]^{\{\varepsilon\}} = L$ (L stands for the preceding interval's left side.) to indicate the evolution of such spiral look. The third spiral appears after the second one and is part of the interval $[20, 40]^{\{\varepsilon\}}$, the fourth to the interval $[40, 60]^{\{\varepsilon\}}$, the fifth to the interval $[60, 80]^{\{\varepsilon\}}$, and the last to the interval $[80, 100]^{\{\varepsilon\}}$.

The coding of this hidden bifurcation route (HBR), which ends with the interval $[-20, 100]^{\{\varepsilon\}}$ is $HBR_{0,4} = [0, 20]^{\{\varepsilon\}}/L/R/R/R/R$ (R stands for the right of the previous interval).

As the value of ε is not important for the search of symmetries of the hidden bifurcation routes, it is omitted and denote simply $HBR_{0,4} = [0, 20]^{\{\varepsilon\}}/L/R/R/R/R$ by $HBR_{0,4} = [0, 20]^{\{\varepsilon\}}/L/R/R/R/R$.

The beginning of the second route (figs. 5.4 and 5.5) is the same ($[0, 20]^{\{\varepsilon\}}/L$). But the third and fourth spirals simultaneously appear, extending the interval. $[-20, 20]^{\{\varepsilon\}}$ to $[-40, 40]^{\{\varepsilon\}}$. Denote this expansion by $[0, 20]^{\{\varepsilon\}} = L = 2Sym$. The fifth and sixth spirals reappear next to the preceding attraction in a symmetrical pattern. The final spiral is a part of the interval. $[60, 80]^{\{\varepsilon\}}$.

The coding of this second route, which ends with the interval $[-60, 80]^{\{\varepsilon\}}$, is $HBR_{2,3} = [0, 20]^{\{\varepsilon\}}/L/2Sym/2Sym/R$ or simply $HBR_{2,3} = [0, 20]^{\{\varepsilon\}}/L/2Sym2/R$.

5.3 Symmetries of the Hidden Bifurcation Routes

For the values of n in eq (4.3), take into account all possible values for p and q , ranging from 3 to 7, and some values of p and q for n between 8 and 12.

5.3.1 Basic Cell

The numerical tests demonstrate that either the coding or the first two spirals come first.

$$([0, 20]^{\{\varepsilon\}}/L)or([-20, 0]^{\{\varepsilon\}}/R),$$

as displayed in figs. 5.6 and 5.7, for the same values of h and k . Therefore, it is called the basic cell and denoted as B , either

$$([0, 20]^{\{\varepsilon\}}/L)or([-20, 0]^{\{\varepsilon\}}/R).$$

The generalized notations used for the coding are B and the following ones:

$$2sym^s = 2Sym/2Sym/\dots/2Sym, \text{ } s \text{ times,}$$

$$L^t = L/L\dots/L, \text{ } t \text{ times,}$$

$$R^u = R/R\dots/R, \text{ } u \text{ times.}$$

5.3.2 Symmetries

For all values of, the hidden bifurcation pathways have all been mathematically calculated. p and q , giving the values of n in eq. (4.3) ranging from 3 to 7. The results ($MARE$ and coded bifurcation routes) are displayed in black color in table 5.1. It was found that

$$MARE_{p,q} = [-20 - 20 \times p, 20 + 20 \times q]. \quad (5.2)$$

Additionally, each hidden bifurcation route's coding is provided by

$$HBR_{p,q} = \begin{cases} B/2sym^s & \text{if } p = q, \\ B/2sym^s / L^{p-s} & \text{if } p > q, \\ B/2sym^s / R^{q-s} & \text{if } p < q, \end{cases} \quad (5.3)$$

which formula controls how many spirals there are and how they appear in the order that they do, where $s = \min(p, q)$. In table 5.1, $HBR_{p,q}$ and $MARE_{p,q}$, which are highlighted in red and match both of the previous formulations (5.2-5.3). It is evident from these numerical findings that the first diagonal exhibits considerable symmetry. This symmetry is defined for $HBR_{p,q}$ by the change of R to L when p is changed in q , and vice versa. Moreover, if $MARE_{p,q} = [a', b']$ then $MARE_{q,p} = [b', a']$.

$\begin{matrix} p \\ \backslash \\ q \end{matrix}$	0	1	2	3	4	5
0		[-40,20]/ B/L	[-60,20]/ B/L/L	[-80,20]/ B/L/L/L	[-100,20]/ B/L/L/L/L	[-120,20]/ B/L/L/L/L/L
1	[-20,40]/ B/R	[-40,40]/ B/2Sym	[-60,40]/ B/2Sym/L	[-80,40]/ B/2Sym/L/L	[-100,40]/ B/2Sym/L/L/L	[-120,40]/ B/2Sym/L ⁴
2	[-20,60]/ B/R/R	[-40,60]/ B/2Sym/R	[-60,60]/ B/2Sym/2Sym	[-80,60]/ /B/2Sym/2Sym/L	[-100,60]/ /B/2Sym ² /L ²	[-120,60]/ B/2Sym ² /L ³
3	[-20,80]/ B/R/R/R	[-40,80]/ B/2Sym/R/R	[-60,80]/ B/2Sym/2Sym/R	[-80,80]/ B/2Sym ³	[-100,80]/ B/2Sym ³ /L ¹	[-120,80]/ B/2Sym ³ /L ²
4	[-20,100]/ B/R/R/R/R	[-40,100]/ R/2Sym/R/R/R	[-60,100]/ B/2Sym ² /R ²	[-80,100]/ B/2Sym ³ /R ¹	[-100,100]/ B/2Sym ⁴	[-120,100]/ B/2Sym ³ /L ¹
5	[-20,120]/ B/R/R/R/R/R	[-40,120]/ B/2Sym ¹ /R ⁴	[-60,120]/ B/2Sym ² /R ³	[-80,120]/ B/2Sym ² /R ²	[-100,120]/ B/2Sym ⁴ /R ¹	[-120,120]/ B/2Sym ⁵

Figure 5.1: Symmetries of the hidden bifurcation routes : $HBR_{p,q}$ and $MARE_{p,q}$, numerically computed (black) and inferred from Eqs. (5.2) and (5.3) (red) }

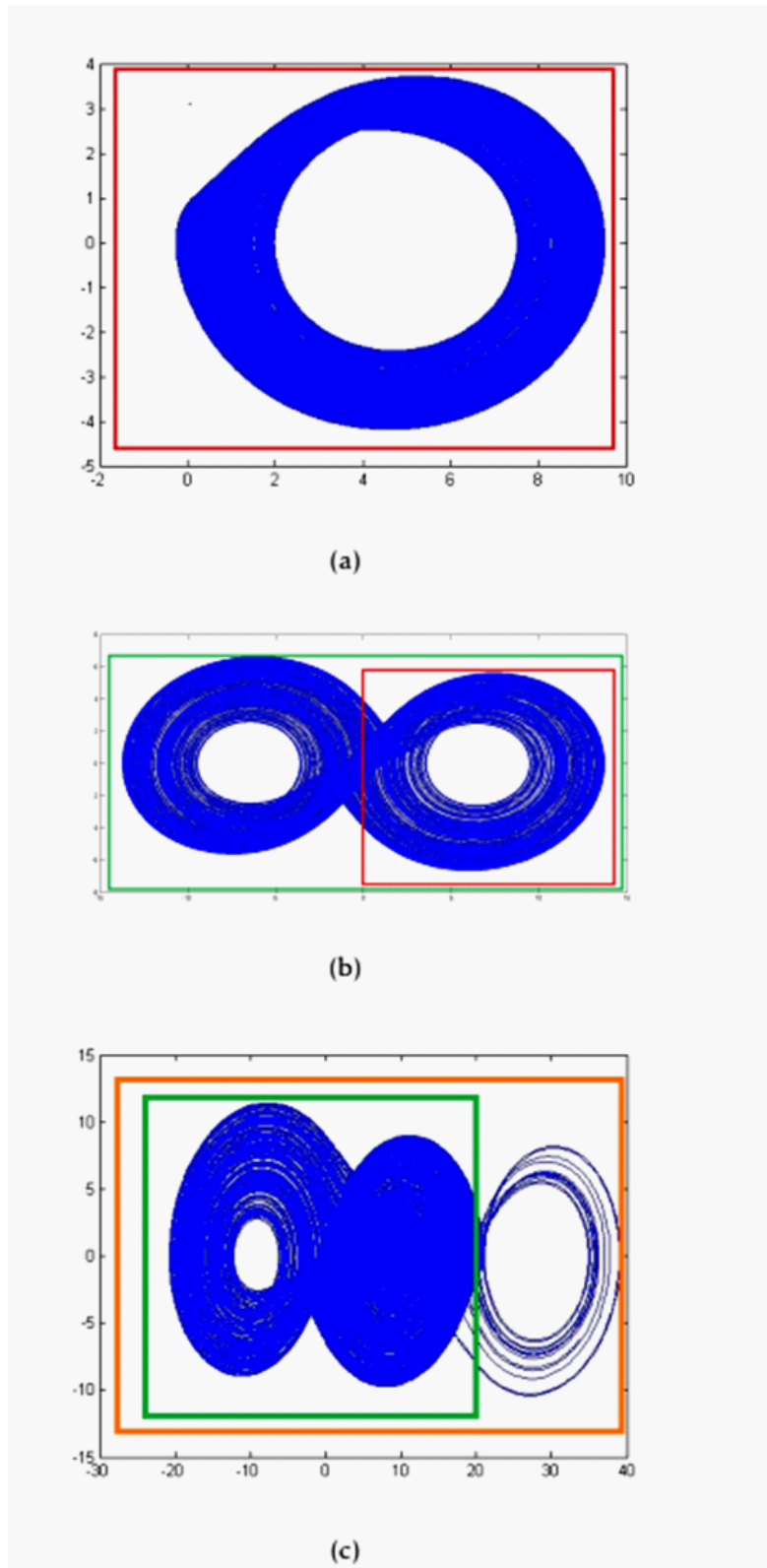


Figure 5.2: The increasing number of spirals of system (4.5) according to increasing ε values, when $p = 0$ and $q = 4$, $k = 10$ and $h = 20$. (a) : The first scroll for $\varepsilon = 0.41$, (b) : The second scroll on the left for $\varepsilon = 0.6$, (c) : the third scroll on the right for $\varepsilon = 0.95$. The horizontal axis is the x-axis, the vertical axis is y-axis.

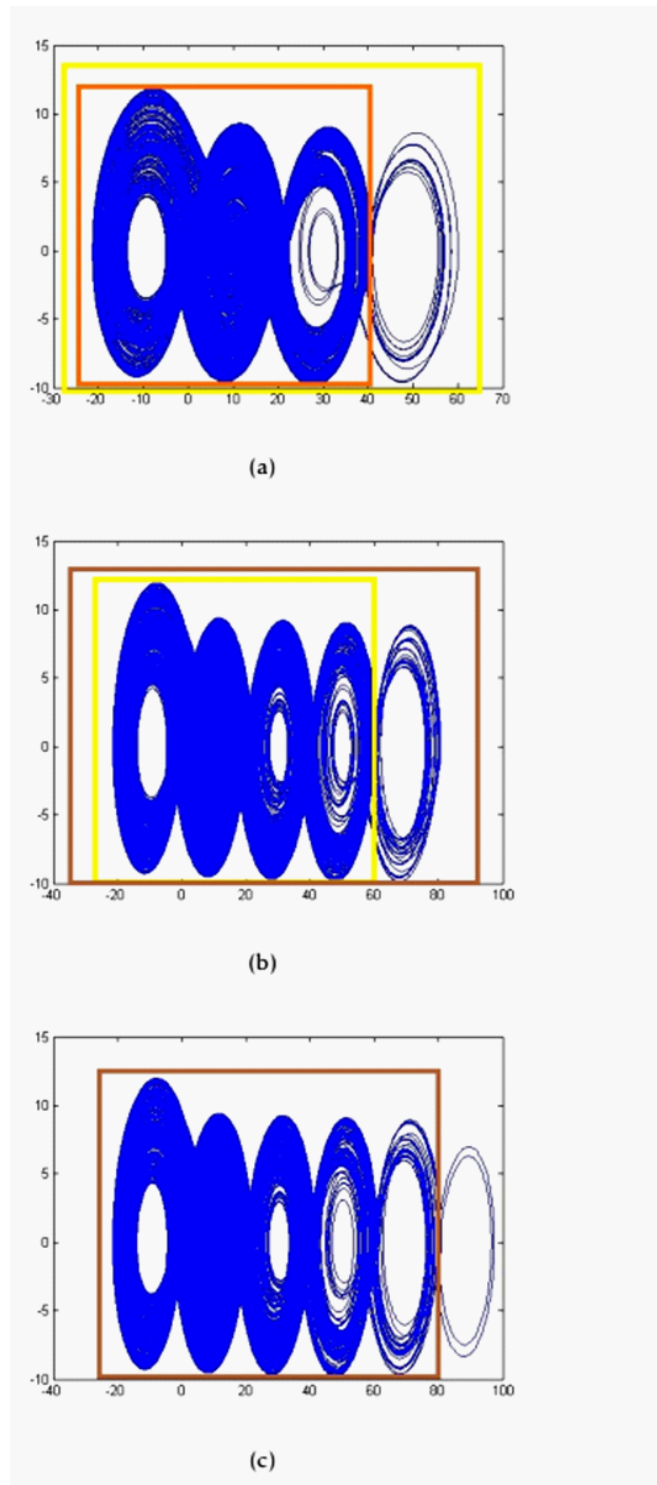


Figure 5.3: The increasing number of spirals of system (4.5) according to increasing ε values, when $p = 0$ and $q = 4$, $k = 10$ and $h = 20$. (a) : The fourth scroll on the right for $\varepsilon = 0.985$, (b) : The fifth scroll on the right for $\varepsilon = 0.988$, (c) : the sixth scroll on the right for $\varepsilon = 0.99$. The horizontal axis is the x-axis, the vertical axis is y-axis

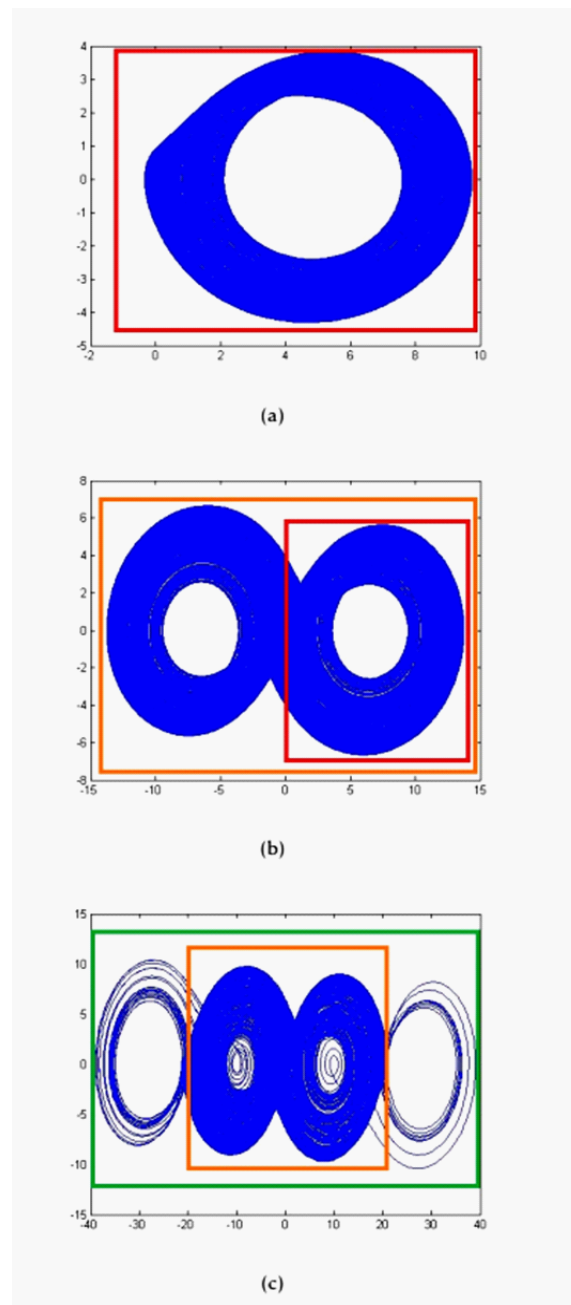


Figure 5.4: The increasing number of scrolls of system (4.5) according to increasing ε values, when $p = 2$ and $q = 3$, $k = 10$ and $h = 20$. (a) : The first scroll on the right for $\varepsilon = 0.42$, (b) : The second scroll on the left for $\varepsilon = 0.6$, (c) : the third and fourth scrolls : two left-right symmetrical for $\varepsilon = 0.95$. The horizontal axis is the x-axis, the vertical axis is y-axis.

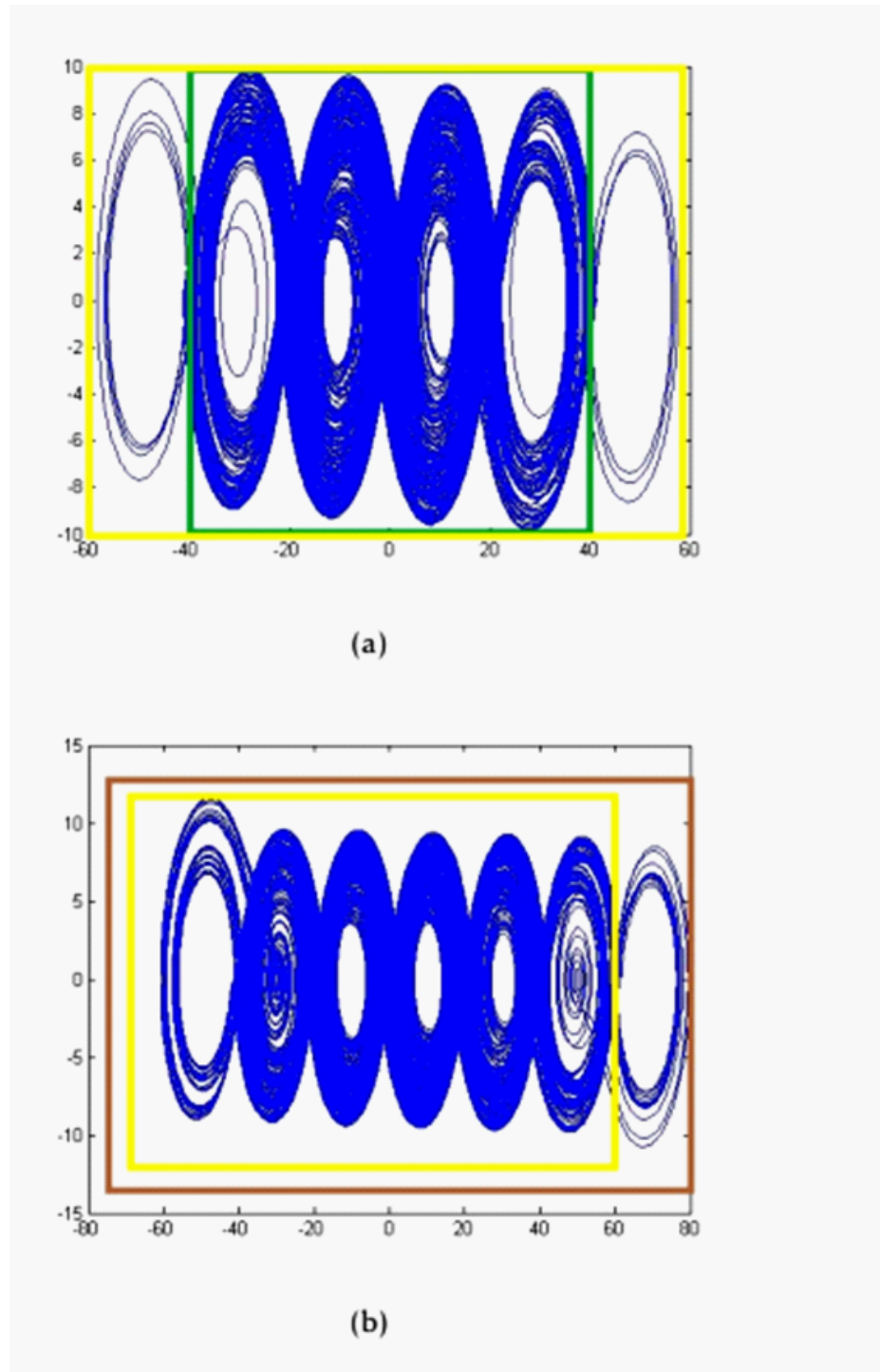


Figure 5.5: The increasing number of spirals of system (4.5) according to increasing ε values, when $p = 2$ and $q = 3$, $k = 10$ and $h = 20$. (a) : The fifth and sixth scrolls : two symmetrical left-right for $\varepsilon = 0.98$, (b) : The seventh scroll on the right for $\varepsilon = 0.99$. The horizontal axis is the x-axis, the vertical axis is y-axis.

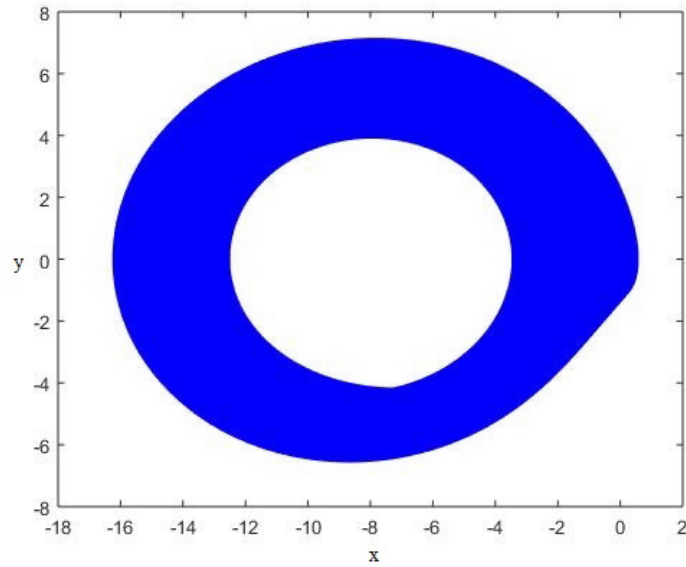


Figure 5.6: The first scroll between -16 and 0 for the values of the parameters $p = 0$ and $q = 4$ with the parameters values $k = 9$ and $h = 18$

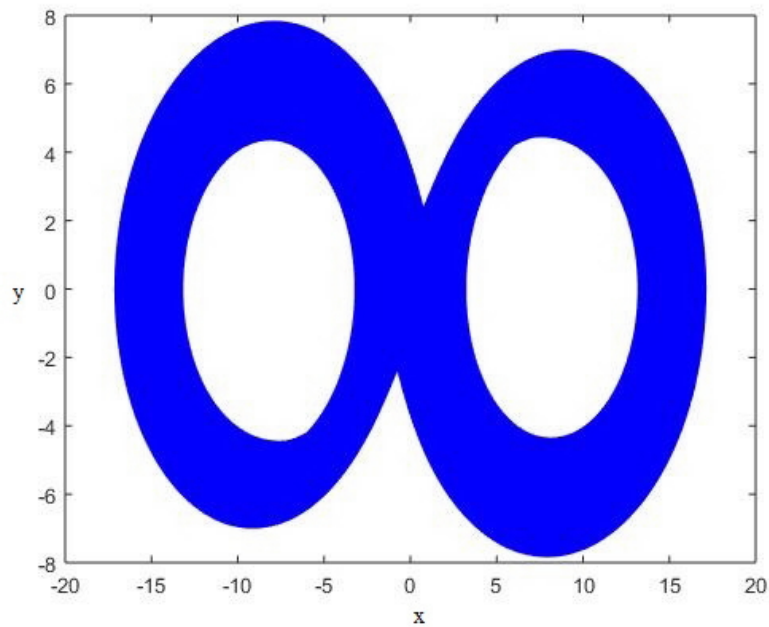


Figure 5.7: The second scroll is in symmetry with the first one, generated between 0 and 20 ($-20, 0$) for the values of the parameters $p = 0$ and $q = 4$ with the parameters values $k = 9$ and $h = 18$

General Conclusion

We have seen in this thesis that attractors and bifurcations of chaotic systems, we divided it into two parts, the first part consists of a preliminary and second chapter on the basic notions of dynamical systems, bifurcation and chaos, a third chapter on hidden attractor their historical, definitions, properties. After that, we presented Leonov method for investigated hidden attractor where the method discovered in 2010. It ends with first application in hidden attractor by Leonov, et al. in chua system. While the second part was devoted to the study, a hidden bifurcation via saturated function serie, first , we presented in fourth chapter a new idea about hidden modalities of spirals of chaotic attractor

where, the gap between these two values ε of grows directly proportionate to the number of spirals. Before finding the asymptotical attractor, for even numbers of spirals, a strategy is employed during the integration operation to have odd or gradually increase the number of spirals until it reaches the maximum number that matches. The value ε promised by the disclosure of an odd number spirals' modalities. The second, we discussed a symmetries in hidden bifurcation routes (*HBR*), the sequence in which the spirals arise under the control of the two parameters and the maximum range extension of their attractors serve as markers for these *HBR*. Interesting symmetries between the two parameters may be seen in these *HBR* as well.

It can be concluded that ,hidden bifurcation a new and good idea for all study where has several applications in various fields such as biology, chemistry, telecommunications

(information security) and physical sciences this has been widely studied in the last seven years. We encountered difficulties in proving our results especially numerical in code Matlab but in last we found the results, it was a perfect results.

Our next project and will be the study of the hidden bifurcation other systems and particular the different systems with other methods.

Bibliography

- [1] M., A. Aizerman. (1949): On a problem concerning the stability in the large of dynamical systems. *Uspekhi Mat. Nauk* 4, 187 – 188 (in Russian).
- [2] A., Al-Obeidi, S.F. Al-Azzawi, M.Thivagar. (2021): A Novel of New 7D Hyperchaotic system with self-excited attractors and Its hybrid synchronization. *Computational Intelligence and Neuroscience*.
- [3] T., A. Alexeeva, N. V. Kuznetsov, T.N. Mokaev. (2021): Study of irregular dynamics in an economic model: attractor localization and Lyapunov exponents. *Chaos Solitons and Fractals*. (152)6275.
- [4] A., Andronov, A. A.Vitt, S. E. Khaikin. (1966): *Theory of oscillators*. (Pergamon, Oxford).
- [5] H., Bao, B.C.Bao, Y.Lin, H.G. Wu. (2016): Hidden attractor and its dynamical characteristic in memristive self-oscillating system. *Acta Phys. Sin.* 65, 1 – 12.
- [6] W., Barnett. (2000): A. Serletis, Martingales, nonlinearity, and chaos, *Journal of Economic Dynamics and Control*. 24, 703 – 724.
- [7] N., N.Bautin. (1939): On the number of limit cycles generated on varying the coefficients from a focus or centre type equilibrium state. *Doklady Akademii Nauk SSSR* 24, 668 – 671 (in Russian).

- [8] N., N.Bautin. (1949): The Behaviour of Dynamical Systems Close to the Boundaries of a Stability Domain (Gostekhizdat, Leningrad, Moscow) [in Russian].
- [9] N., N.Bautin. (1952): On the number of limit cycles appearing on varying the coefficients from a focus or centre type of equilibrium state. *Mat. Sb. (N.S.)* 30, 181 – 196 (in Russian).
- [10] M., Belouerghi, T. Menacer, R. Lozi. (2019): Hidden patterns of even number of spirals of chua chaotic attractor unveiled by a novel integration duration based method, *Indian Journal of Industrial and Applied Mathematics.* 3(4), 0973 – 1002.
- [11] S., Boccaletti, C. Grebogi, Y. C. Lai, H. Mancini, D. Maza. (2000): The control of chaos: Theory and applications, *Physics Reports.* 329(3), 103 – 197.
- [12] V., H. Carbajal-Gomez, E. Tlelo-Cuautle, J. M. MuñozPacheco, L. G. de la Fraga, C. Sanchez-Lopez, F. V. Fernandez-Fernandez. (2019): Optimization and CMOS design of chaotic oscillators robust to PVT variations,” *Integration.* 65, 32 – 42.
- [13] L., Chua L, Komuro M, Matsumoto T. (1986): The Double Scroll Family. *IEEE Trans Circuits Syst.* 33(11), 1072 – 118.
- [14] Q., Deng, C.Wang. (2019): Multiscroll hidden attractors with two stable equilibrium points. *Chaos* 29, 093112.
- [15] D., Dudkowski, S. Jafari, T.Kapitaniak, N. V. Kuznetsov, G., A. Leonov, A.Prasad. (2016): Hidden attractors in dynamical systems. *Physics Reports,* 637, 1 – 50.
- [16] J., Guckenheimer, P. Holmes. (1983): Non linear oscillations, dynamical systems and bifurcation of vector fields. Springer-Verlag.
- [17] D., Hilbert.(1902): Mathematical problems. *Bull. Am. Math. Soc.*8, 437 – 479.

- [18] G., Hu. (2009): Generating hyperchaotic attractors with three positive Lyapunov exponents via state feedback control. *International Journal of Bifurcation and Chaos*. 19(2), 651 – 660.
- [19] M., Kapranov. (1956): Locking band for phase-locked loop. *Radiofizika*. 2, 37 – 52 (in Russian).
- [20] M., A. Kiselevaa, E. V. Kudryashova, N. V. Kuznetsova, O. A. Kuznetsova, G. A. Leonova, M. V. Yuldashev, R. V. Yuldasheva.(2017): Hidden and self-excited attractors in Chua circuit : synchronization and SPICE simulation.*International journal of parallel, emergent and distributed systems*.
- [21] M., Kiseleva, N. Kuznetsov, G. Leonov. (2016): Hidden attractors in electromechanical systems with and without equilibria, *IFAC-PapersOnLine*. 49(14), 51 – 55.
- [22] Y., Kuznetsov. (1998): *Elements of Applied Bifurcation Theory*. Second Edition. Springer-Verlag New York, Inc.
- [23] N., Kuznetsov, V. Reitmann. (2021): *Attractor Dimension Estimates for Dynamical Systems: Theory and Computation (Dedicated to Gennady Leonov)*, Springer, Cham.
- [24] N., Kuznetsov. (2020): Theory of hidden oscillations and stability of control systems, *Journal of Computer and Systems Sciences International*. 59(5), 647 – 668.
- [25] N., Kuznetsov, T. Mokaev, O. Kuznetsova, E. Kudryashova. (2020): The Lorenz system: hidden boundary of practical stability and the Lyapunov dimension, *Nonlinear Dynamics*. 102, 713 – 732.
- [26] N., Kuznetsov, G. Leonov, T. Mokaev, A. Prasad, M. Shrimali. (2018): Finite-time Lyapunov dimension and hidden attractor of the Rabinovich system, *Nonlinear Dynamics*. 92(2), 267 – 285.

- [27] G., A. Leonov, N. V. Kuznetsov. (2011): Localization of hidden Chua's attractors. *Phys. Lett. A*, 375, 2230 – 2233.
- [28] G., A. Leonov. (2010): Effective methods for periodic oscillations search in dynamical systems. *Appl. Math. Mech*, 74, 37 – 73.
- [29] G., A. Leonov, V.I. Vagaitaev, N. V. Kuznetsov. (2010): Algorithm for localizing Chua attractors based on the harmonic linearization method. *Dokl. Math*, D, 663 – 666.
- [30] G., A. Leonov, N. V. Kuznetsov. (2011): Analytical numerical methods for investigation of hidden oscillations in nonlinear control systems. *Proc. 18th IFACWorld Congress*, Milano, Italy, August, 28, 2494 – 2505.
- [31] G., A. Leonov, N. V. Kuznetsov, V.I. Vagaitaev. (2012): Hidden attractor in smooth Chua systems. *Physica D*, 241, 1482 – 1486.
- [32] G., A. Leonov, N. V. Kuznetsov. (2013): Hidden Attractors in Dynamical Systems. *International Journal of Bifurcation and Chaos*, 23, (1330002 – 1330071).
- [33] G., Leonov, N. Kuznetsov, T. Mokaev. (2015): Homoclinic orbits, and self-excited and hidden attractors in a Lorenz-like system describing convective fluid motion, *The European Physical Journal Special Topics*. 224(8), 1421 – 1458.
- [34] E., N.Lorenz. (1963): Deterministic nonperiodic flow. *J. Atmos. Sci.* 20, 130 – 141.
- [35] J., Lü, G. Chen. (2006): Generating multiscroll chaotic attractors: Theories, methods and applications. *International Journal of Bifurcation and Chaos*, 16(4), 775 – 858.
- [36] J., Lü, G. Chen. X. YU, H. LEUNG. (2004): Design and analysis of multiscrollchaotic attractors from saturated function series. *IEEE Trans. Circuits Syst. I*, 51(12), 2476 – 2490.

- [37] N.,A.Magnitsikii, S.V.Sidorov. (2006): New methods for Chaotic dynamic.World Scientific Publishing Co. Pte. Ltd.
- [38] T., Menacer. (2009): Synchronisation des systèmes dynamiques chaotiques à dérivées fractionnaires. Memoire de doctorat. University Mentouri Constantine.
- [39] T., Menacer, R. Lozi, L .O Chua. (2016): Hidden bifurcations in the multispiral Chua attractor. International Journal of Bifurcation and Chaos,16(4), 1630039 – 1630065.
- [40] A., Menasri. (2015): Chaos et bifurcations dans les systèmes dynamiques en dimensions $n(n > 1)$. Memoire de doctorat. University Larbi Bin M'Hidi.
- [41] A.,E. Mohamed Salah. (2009): Les systems chaotiques à dérivées fractionnaires. Memoire de doctorat. University Mentouri Constantine.
- [42] H., Poincaré. (1885): L'Equilibre d'une masse fluide anim'ee d'un mouvement de rotation, Acta Mathematica. 7, 259 – 380.
- [43] V.,T. Pham, S.Vaidyanathan, C.K. Volos, S. Jafari. (2015): Hidden attractors in a chaotic system with an exponential nonlinear term. Eur. Phys. J. Special Topics. 224, 1507 – 1517.
- [44] J., W. S. Rayleigh. (1877): The Theory of Sound. (MacMillan, London).
- [45] O.E., Rossler. (1976): An equation for continuous chaos. Phys. Lett. A, 57, 5, pp. 397 – 398.
- [46] C.,Rousseau. (1989): Codimension 1 and 2 bifurcations of fixed points of diffeomorphisms and periodic solutions of vector fields. Ann. SC. math. Québec, 13(2), 55 – 91.
- [47] D.,Ruelle, F.Takens. (1971): On the nature of turbulence. Commun. Math. Phys., 20(3), 167 – 192.

- [48] J.,Sajad, J.C. Sprott. (2013): Elementary quadratic chaotic flows with no equilibria. *Phys. Lett. A* 377, 699 – 702.
- [49] J.,A. Suykens, J. Vandewalle. (1993): Generation of n-double scrolls ($n = 1, 2, 3, 4, \dots$). *IEEE Trans. Circuits Syst.*40(I), 861 – 867.
- [50] J.,A. Suykens, R. Oberoi. (1997): A family of n-scroll attractors from a generalized Chua's circuit. *Int. J. Electron. Commun*, 51(3), 131 – 138.
- [51] N.,V.Stankevich N.V.Kuznetsov, G.A. Leonov, L.O. Chua. (2017): Scenario of the Birth of Hidden Attractors in the Chua Circuit. *Int J Bifurcation Chaos*. 27(12), 1730038.
- [52] E., Tlelo-Cuautle, J. J. Rangel-Magdaleno, A. D. Pano-Azucena, P. J. Obeso-Rodelo, and J. C. Nuñez-Perez. (2015): FPGA realization of multi-scroll chaotic oscillators. *Communications in Nonlinear Science and Numerical Simulation*. 27(1), 66 – 80.
- [53] F., Verhulst. (1990): Non linear Differential equations and Dynamical systems. *Springe-Verlag Berlin Heidelberg*.
- [54] X.,Wang, G.R. Chen. (2012): A chaotic system with only one stable equilibrium. *Commun. Nonlinear Sci. Numer.Simulat*. 17, 1264 – 1272.
- [55] S.,Wang, Ch. Wang, C. Xu. (2020): An image encryption algorithm based on a hidden attractor chaos system and the Knuth-Durstenfeld algorithm, *Optics and Lasers in Engineering*, 128, 105995.
- [56] X.,Wu, H.wang, S.He. (2021): Localization of hidden attractors in Chua's system with absolute nonlinearity and Its FPGA implementation. *Frontiers in Physics*. 9, 788329.
- [57] M., E. Yalcin, J. A. S. Ozogus, J.,A. Suykens, J. Vandewalle. (2001): n-scroll chaos generators: A simple circuit model. *Electron. Lett*, 37(3), 147 – 148.

- [58] F., Zaamoune, T. Menacer, R. Lozi, G. Chen. (2019): Symmetries in hidden bifurcation routes to multiscroll chaotic attractors generated by saturated function series, *Journal of Advanced Engineering and Computation*, 3(4), 511 – 522.
- [59] F., Zaamoune, T. Menacer. (2022): Hidden modalities of spirals of chaotic attractor via saturated function series and numerical results. *Analysis and mathematical physics*. 12(5), 1664 – 1685.
- [60] H., Zhao, Y. Lin, Y.Dai. (2014): Hidden Attractors and Dynamics of a General Autonomous van der Pol-Duffing Oscillator. *Int J Bifurcation Chaos*. 24(06), 1450080.
- [61] E.,Zeraoulia. (2006): Etude de quelques types de systems chaotique : generalisation d'un modele issu du model Chen. Memoire de doctorat. University Mentouri Constantine.
- [62] G., Zhang, F. Zhang, X. Liao, D. Lin, P. Zhou. (2017): On the dynamics of new 4D Lorenz-type chaos systems,” *Advances in Difference Equations*. (1), 13 page.
- [63] X., Zhang, Ch. Wang. (2019): A novel multi-attractor period multi-scroll chaotic integrated circuit based on CMOS wide adjustable. *CCCII, IEEE Access*, 7(1), 16336 – 16350.
- [64] X., Zhang, C. Wang. (2019): Multiscroll hyperchaotic system with hidden attractors and its Circuit implementation, *International Journal of Bifurcation and Chaos*, 29(09), 1950117.
- [65] S.,Zhang, Y.Zeng, Z. Li, M. Wang, L. Xiong L. (2018): Generating One to Four-wing Hidden Attractors in a Novel 4d No-Equilibrium Chaotic System with Extreme Multistability. *Chaos*. 28(1), 013113.
- [66] D.,Zhang, F,Li. (2022): Chaotic dynamics of non-autonomous nonlinear system for a sandwich plate with truss core. *Mathematics*, 1889(10).

- [67] Ch.,Zhang, Q.Tang. (2022): Complex periodic mixed-mode oscillation patterns in a flippov system. *Mathematics*, 673(10).
- [68] L., Zhou, Ch. Wang, Li. Zhou. (2016): Generating hyperchaotic multi-wing attractor in a $4D$ memristive circuit. *Nonlinear Dynamics*. 85(4), 2653 – 2663.
- [69] W.,Zhou, F.Yuan. (2018): Hidden coexisting attractors in choatic system without equilibrium point. *International Journal of Bifurcation and Chaos*.
- [70] L., Zhou, Ch. Wang, Li. Zhou. (2018): A novel no-equilibrium hyperchaotic multi-wing system via introducing memristor. *International Journal of Circuit Theory and Applications*, 46(1), 84 – 98.

Annexe A: Program in MATLAB for Hidden Bifurcation Saturated Function Series.

```
function dy = Essa5i(~,y)
a=0.7;
b=0.7;
c=0.7;
d1=0.;
k=10;
p=2;
q=2;
h=20;
%s=14.0;
%a2=0.8;
%b2=0.72;
%c2=0.6;
k1=-0.33;
eps =1;
if y(1)<-p*h-1
```

```
H= -(2*p+1)*k;
end
for i=-p: q-1
if (y(1)>i*h+1)& & (y(1)<(i+1)*h-1)
H= (2*i+1)*k;
end
end
for i=-p: q
if abs(y(1)-i*h)<=1
H= k*(y(1)-i*h)+2*i*k;
end
end
if y(1) > q*h+1
H=(2*q+1)*k;
end
dy = double(zeros(3,1)); % a column vector
dy(1) =y(2);
dy(2) =y(3);
dy(3) = -a*y(1)-b*y(2)-c*y(3)+k1*d1*y(1)+eps*d1*H-eps*k1*d1*y(1);
%dy(3) =-a*y(1)-b*y(2)-c*y(3)+d1*H;
end
%1/s*y
%(-x+r*y-r*y*z^2)/(1+w^2)
%-y-b*z+z*y
%-y-c*w+w*y
```

```
clear all
close all
clc
options = odeset('AbsTol',1e-11,'RelTol',1e-6);
%C=10a?=x?=39.97;y?=39.97×0.031084 = 1.2424, z? = 39.97 × (-1.2946) = -51.745
%C=8a?=x?=31.99;y?=31.99×0.031084 = 0.99438, z? = 31.99 × (-1.2946) = -41.414
%C=2a?=x?=8.13;y?=8.13×0.031084 = 0.25271z? = 8.13 × (-1.2946) = -10.525
%C=4a?=x?=16.05;y?=16.05×0.031084 = 0.49890, z? = 16.05 × (-1.2946) = -20.778
%c=1 (2-scroll),x(0)=4.22,y(0)=0.13117,z(0)=-5.4632
%C=3x(0)=12.09 ,y(0)=0.37581,z(o)=-15.652.
%c=6 (7-scroll) ? x(0)=24, y(0)=0.74602,z(0)=-31.07
%C=5a?=x?=20.02;y?=20.02×0.031084 = 0.6223, z? = 20.02 × (-1.2946) = -25.918.
%C=7,C=x(0)=28 ,y(0)=0.87035,z(o)=-36.249.
%C=9,C=x(0)=36 ,y(0)=1.119,z(o)=-46.606.
%C=11a?=x?=43.95;y?=1.3661=,z?=-56.898
%C=12a?=x?=47.95;y?=47.95×0.031084 = 1.4905, z? = 47.95 × (-1.2946) = -62.076
%[T1,Y] = ode45(@Chuanew3,[0 30000],[47.95 1.4905 -62.076],options);%c=12
%[T1,Y] = ode45(@Chuanew3,[0 100000],[39.97 1.2424 -51.745],options);%c=10
%[T1,Y] = ode45(@Chuanew3,[0 100000],[31.99 0.99438 -41.414],options);%c=8
%[T1,Y] = ode45(@Chuanew3,[0 100000],[24 0.74602 -31.07],options);%c=6
%[T1,Y] = ode45(@Chen3,[0 5000],[12.09 0.37581 -15.652],options);%c=3
%[T1,Y] = ode45(@Chuanew3,[0 50000],[16.05 0.49890 -20.778],options);%c=4
%[T1,Y] = ode45(@Chen3,[0 10000],[8.13 0.25271 -10.525],options);%c=2
%[T1,Y] = ode45(@Chuanew3,[0 350000],[43.95 1.3661 -56.898],options);%c=11
[T1,Y] = ode45(@Essa5i,[0 1500000],[10.8914 3.6739 -2.1975],options); %c==1
%[T1,Y] = ode45(@Chuanew3,[0 10000],[12.09 0.37581 -15.652],options);%c=6
%[T1,Y] = ode45(@Chuanew3,[0 10000],[20.02 0.6223 -25.918],options);%c=5
```

```
%[T1,Y] = ode45(@Chuanew3,[0 100000],[28 0.87035 -36.249],options);%c=7
%[T1,Y] = ode45(@Chuanew3,[0 10000],[36 1.119 -46.606],options);%c=9
%plot(T2,YY(:,1),'-',T,YY(:,2),'-.',T,YY(:,3),'.')
N=size(Y);
nm=round(9*N(1)/10);
for i=1:N(1)-nm
y1(i)=Y(i+nm,1);y2(i)=Y(i+nm,2);y3(i)=Y(i+nm,3);
end
yy=Y(N(1),:)
%figure(1)D
%plot3(y1,y2,y3,'b');grid
%figure(2)
%for i=0:2
% xe1=4*1.3*i;
% ye1=0;
% ze1=-xe1;
%hold on
%plot(xe1,ye1,'*r')
% xe2=-4*1.3*i;
%ye2=0;
%ze2=-xe2;
%hold on
%plot(xe2,ye2,'*r')
%end
%hold on
%plot(y1,y2,'b')% μfigure(3)
%plot(y1,y2,'r')
```

```
figure(4)
plot(y1,y2,'b')
figure(5)
plot(y2,y3,'b')
figure(6)
plot3(y1,y2,y3,'b')
figure(8)
plot(y1,y3,'b')
%figure(3)
%plot(Y(:,1),Y(:,3),'b');grid
%figure(4)
%plot(Y(:,2),Y(:,3),'b');grid
```



Abstract

The hidden bifurcation idea was discovered by the core idea of the Leonov and Kuznetsov method for searching hidden attractors (i.e., homotopy and numerical continuation) differently in order to uncover hidden bifurcations governed by a homotopy parameter ε while keeping the numbers of spirals. This idea was first discovered by Menacer et al. In 2016, in the multispiral Chua system,

The first part of this thesis is devoted to providing a basic understanding of dynamic systems and chaos, followed by an introduction to the hidden attractors, history, and definitions. An effective procedure for the numerical localization of hidden attractors in multidimensional dynamical systems has been presented by Leonov et Kuznetsov. In this part, we end with the study of hidden attractors in the Chua system.

The second part of the analysis consists of first, hidden modalities of spirals of chaotic attractor via saturated function series and numerical results. Before reaching the asymptotic attractor which possesses an even number of spirals, these latter are generated one after one until they reach their maximum number, matching the value fixed by ε . Then, we end up by symmetries in hidden bifurcation routes to multi-scroll chaotic attractors generated by saturated function series. The method to find such hidden bifurcation routes (HBR) depends upon two parameters.

Key-words

Dynamical Systems, Chaos, Hidden attractors, Hidden bifurcation, modality of an odd number of spirals, Saturated function series, multi-spirals chaotic attractor, Symmetry.



Résumé

L'idée de bifurcation cachée a été découverte par l'idée centrale de la méthode de Leonov et Kuznetsov pour rechercher différemment les attracteurs cachés (c'est-à-dire l'homotopie et la continuation numérique), afin de découvrir les bifurcations cachées, régies par un paramètre d'homotopie ε tout en gardant le nombre de spirales, cette idée a été découverte par Menacer et al. En 2016 dans le système Chua multispirale.

La première partie de cette thèse est consacrée à fournir une compréhension de base des systèmes dynamiques et du chaos, suivie d'une introduction aux attracteurs cachés, à l'histoire et aux définitions. Une procédure efficace pour la localisation numérique des attracteurs cachés dans les systèmes dynamiques multidimensionnels a été présentée par Leonov et Kuznetsov. Dans cette partie, nous terminons par l'étude des attracteurs cachés dans le système Chua.

La deuxième partie analyse, d'abord, les modalités cachées des spirales d'attracteur chaotique via des séries de fonctions saturées et des résultats numériques c'est l'opération d'intégration, avant d'atteindre l'attracteur asymptotique qui possède un nombre pair de spirales, ces dernières sont générées une à une jusqu'à ce qu'elles atteignent leur nombre maximum correspondant à la valeur fixée par ε . et nous nous retrouvons par des symétries dans les routes de bifurcation cachées vers des attracteurs chaotiques multi-scroll générés par des séries de fonctions saturées, la méthode pour trouver de telles routes de bifurcation cachées (HBR) dépendant de deux paramètres.

Mot clés :

Systèmes dynamiques, Chaos, Attracteurs cachés, Bifurcation cachée, Modalité d'un nombre impair de spirales, Séries de fonctions saturées, Attracteur chaotique multi-spirales, Symétrie.

الملخص

تم اكتشاف فكرة التشعب المخفي من خلال الفكرة الأساسية لطريقة ليونوف وكوزنيتسوف للبحث عن الجاذبات المخفية (أي الاستمرارية العددية والتمثيلية) بشكل مختلف ، من أجل الكشف عن التشعبات المخفية ، التي تحكمها معلمة تماثلية ϵ مع الاحتفاظ بأعداد اللوالب ، وهذا تم اكتشاف الفكرة لأول مرة بواسطة Menacer et al. في عام 2016 في نظام Chua متعدد الحلقات.

تم تخصيص الجزء الأول من هذه الأطروحة لتوفير فهم أساسي للأنظمة الديناميكية والفوضى تليها مقدمة للجاذبين المخفيين والتاريخ والتعريفات. تم تقديم إجراء فعال للتوطين العددي للجاذبات الخفية في الأنظمة الديناميكية متعددة الأبعاد بواسطة Leonov et Kuznetsov. في هذا الجزء ، نختتم بدراسة الجاذبات الخفية في نظام تشوا.

الجزء الثاني تحليل ، أولاً ، الطرائق المخفية للحلزونات من الجاذب الفوضوي عبر سلسلة الوظائف المشبعة والنتائج العددية هي عملية التكامل ، قبل الوصول إلى الجاذب المقارب الذي يمتلك عددًا زوجيًا من اللوالب ، يتم إنشاء هذه الأخيرة واحدة تلو الأخرى حتى تصل الحد الأقصى لعدد المطابقة للقيمة المحددة بواسطة ϵ . وننتهي من خلال التماثلات في مسارات التشعب المخفية لجاذبات فوضوية متعددة التمرير تم إنشاؤها بواسطة سلسلة الوظائف المشبعة ، وهي طريقة للعثور على مسارات التشعب المخفية (HBR) اعتمادًا على معلمتين.

الكلمات المفتاحية

الأنظمة الديناميكية ، الفوضى ، الجاذبات الخفية ، التشعب المخفي ، طريقة عدد فردي من الحلزونات ، سلسلة الوظائف المشبعة ، الجاذب الفوضوي متعدد التمرير ، التناظر.